https://doi.org/10.5194/egusphere-2024-1597
Preprint. Discussion started: 27 June 2024

Projections of Precipitation and Temperatures in Greenland and the Impact of Spatially Uniform Anomalies on the Evolution of the Ice Sheet

Nils Bochow[1,2], Anna Poltronieri[1], and Niklas Boers[2,3,4]

[1]Department of Mathematics & Statistics, Faculty of Science and Technology, UiT – The Arctic University of Norway, Tromsø, Norway.
[2]Potsdam Institute for Climate Impact Research, Potsdam, Germany.
[3]Earth System Modelling, School of Engineering & Design, Technical University of Munich, Germany.
[4]Department of Mathematics and Global Systems Institute, University of Exeter, UK.

Correspondence: Nils Bochow (nils.bochow@uit.no)

Abstract. Long-term simulations of the Greenland ice sheet (GrIS) often rely on parameterisation schemes for the precipitation rates or assume spatially and temporally uniform temperature and precipitation anomalies over long time scales. However, there is no a priori reason to assume spatially and temporally uniform sensitivities across the whole GrIS. Additionally, parameters are often based on older generations of climate models and it is often assumed that precipitation increases with the standard value of circa 7%/K based on the Clausius-Clapeyron relation. Here, we give an update on the commonly used parameters used for long-term modelling of the Greenland ice sheet, based on the output of the latest generation of coupled Earth system models (CMIP6), using the historical time period and four different future emission scenarios. We show that the precipitation sensitivities in Greenland have a strong spatial dependence, with values ranging from 0%/K in southern Greenland up to 15%/K in northeastern Greenland relative to the global mean temperature (GMT) in the CMIP6 ensemble mean. Additionally, we show that the annual mean temperatures in Greenland increase between 1.29 and 1.53 times faster than the GMT, with northern Greenland warming up to two times faster than southern Greenland in all emission scenarios. However, we also show that there is a considerable spread in the model responses. Finally, we use the state-of-the-art ice sheet model PISM to show that assuming spatially uniform temperature and precipitation anomalies leads to substantial overestimation of ice loss in the long-term behaviour of the GrIS.

1 Introduction

The Greenland ice sheet (GrIS) is the second largest terrestrial ice sheet with the potential of more than 7.4 m of sea level rise when completely melted (Morlighem et al., 2017). Increasing atmospheric and oceanic temperatures due to climate change (Straneo and Heimbach, 2013; Fettweis et al., 2017) led to more than a 5-fold increase in ice loss from the Greenland ice sheet in the last three decades (Shepherd et al., 2020; Otosaka et al., 2023). Land ice melt already contributed more than half of the global sea level rise since 1993 with an acceleration in recent years (Edwards et al., 2021). The mass balance of the GrIS, i.e. the difference between accumulation and ablation, has been decreasing steadily in the last decades, with an average yearly mass

https://doi.org/10.5194/egusphere-2024-1597
Preprint. Discussion started: 27 June 2024

loss of 169 ± 9 Gt/yr between 1992 and 2020. This caused a cumulative global sea level rise of more than 12 mm (Shepherd et al., 2020; Otosaka et al., 2023). The decrease in mass balance of the GrIS in the last decades is divided approximately equally between discharge due to ice dynamics and increased surface melt (van den Broeke et al., 2009; Choi et al., 2021). However, projections show that increases in Greenland surface melt will dominate the decrease of the mass balance in the long-term (Goelzer et al., 2020; Choi et al., 2021; Payne et al., 2021).

Many studies have investigated the past and future evolution of the Greenland ice sheet from short to long timescales, using computational methods ranging from simple conceptual models (Levermann and Winkelmann, 2016; Boers and Rypdal, 2021), stand-alone ice sheet models (Bochow et al., 2023), Earth system models of intermediate complexity with dynamically coupled ice sheets (Robinson et al., 2012; Gregory et al., 2020; Höning et al., 2023, 2024), to full Earth system models (ESMs) (Muntjewerf et al., 2020a, b; Madsen et al., 2022). In the latest generation of comprehensive ESMs the ice sheets were not fully bidirectionally coupled to the other components, however recently dynamically coupled ice sheets have successfully been introduced in several ESMs (Muntjewerf et al., 2020b; Smith et al., 2021). While this coupling is making rapid progress, parameterisation schemes are still needed, especially to investigate the long-term behaviour of the ice sheets. Computational constrains make it currently virtually impossible to run ESMs on millennial or even decamillennial timescales.

Two of the most commonly used parameterisation approaches in long-term ice sheet modelling are (1) the use of a fixed precipitation increase per degree of temperature increase (e.g., Saito et al., 2016; Aschwanden et al., 2019; Rodehacke et al., 2020; Garbe et al., 2020; Albrecht et al., 2020; Zeitz et al., 2022; Bochow et al., 2023) and (2) the use of scalar temperature anomalies (e.g., Robinson et al., 2012; Aschwanden et al., 2019; Garbe et al., 2020; Zeitz et al., 2022; Bochow et al., 2023).

The expected increase in precipitation with increasing surface temperatures is based on the Clausius-Clapeyron relationship (Clausius, 1850), which describes the increase of the saturation water vapour pressure with increasing temperature according to

$$\frac{\mathrm{d}e_s}{\mathrm{d}T} = \frac{L(T)e_s}{RT^2}\,, \tag{1}$$

with the saturation vapour pressure e_s, the temperature T, the specific latent heat of evaporation of water $L(T = 0°\mathrm{C}) = 2.5 \cdot 10^6\,\mathrm{Jkg}^{-1}$ (Henderson-Sellers, 1984), and the specific gas constant for water vapour $R = 462\,\mathrm{JK}^{-1}\,\mathrm{kg}^{-1}$. The saturation water vapour pressure thus increases approximately exponentially with temperature. Assuming the precipitation P is solely governed by the saturation water vapour pressure, then also P is expected to increase exponentially. Using the chain rule, Equation 1 can be rewritten as

$$k = \frac{\mathrm{d}\ln(e_s)}{\mathrm{d}T} = \frac{L(T)}{RT^2}, \tag{2}$$

with the growth constant k.

For inland Greenland the approximate annual inland near-surface temperature between 1996 and 2019 is $-23°\mathrm{C}$ (Jiang et al., 2020). Plugging the given values into Equation 2 gives $k = 0.086\,1/\mathrm{K}$, which corresponds to a precipitation sensitivity of approximately 9%/K.

In the literature a precipitation sensitivity between 4 and 8%/K is commonly used for simulating the future evolution of the Greenland ice sheet (Huybrechts, 2002; Robinson et al., 2012; Frieler et al., 2015; Saito et al., 2016; Goelzer et al., 2020;

https://doi.org/10.5194/egusphere-2024-1597
Preprint. Discussion started: 27 June 2024

Zeitz et al., 2021; Aschwanden et al., 2019; Zeitz et al., 2022; Bochow et al., 2023). However, these values are often based on older generations or a limited selection of climate models (Robinson et al., 2012; Frieler et al., 2015; Aschwanden et al., 2019; Zeitz et al., 2022; Zhang et al., 2024), and sensitivities are derived using inappropriate regions for Greenland. For example, they often include Iceland or parts of Canada, which can substantially influence the sensitivity (Frieler et al., 2012). Additionally, the precipitation parameterisation as well as scalar temperature anomalies assume that there is a uniform change of temperatures and precipitation rates across Greenland, which is not necessarily true. It has been shown using observations and models that, regionally, the deviations from the thermodynamic expectation around 7%/K can be highly significant (Traxl et al., 2021; Nicola et al., 2023).

Here, we give an update on some commonly used parameterisation factors, informed by the projections of the ESMs that participated in the 6th phase of the coupled model intercomparison project (CMIP6). We analyse temperature and precipitation changes in Greenland from the year 1850 to 2100 for four future emission scenarios (SSP1-2.6, SSP2-4.5, SSP3-7.0 and SSP5-8.5) using the CMIP6 ensemble. Based on this analysis, we derive scalar and spatially resolved temperature scaling factors and precipitation sensitivities for Greenland. Subsequently, we show the difference between using spatially uniform and spatially resolved temperature and precipitation anomalies for the short- and long-term evolution of the GrIS, using the Parallel Ice Sheet Model (PISM) with the simple diurnal energy balance model dEBM-simple (Winkelmann et al., 2011; Zeitz et al., 2021).

2 Data and methods

2.1 CMIP6

We utilise 32 models of the Coupled Model Intercomparison Project Phase 6 (CMIP6), which were all the models that could be downloaded during the data collection (see Appendix). In addition to the historical runs, we use the four Shared Socio-economic Pathways (SSP) scenarios, 1-2.6 (Low challenges to mitigation and adaptation), 2-4.5 (Medium challenges to mitigation and adaptation), 3-7.0 (High challenges to mitigation and adaptation) and 5-8.5 (High challenges to mitigation, low challenges to adaptation) (Riahi et al., 2017), where the last two digits denote the forcing level in $10 \cdot \mathrm{W/m^2}$.

We analyse the model-specific and ensemble mean of the historical (1850-2015) and future atmospheric near-surface temperature (tas) and precipitation (pr) changes in Greenland until the year 2100. For the analysis, we regrid all models to a common gaussian grid with a resolution of $0.5° \times 0.5°$ using a bilinear grid interpolation, using the cdo command line tools (Schulzweida, 2023). For all models, we define Greenland as the geopandas area *Greenland* with a buffer distance of 0.5 corresponding to approximately 50 km (Jordahl et al., 2020). With this approach we avoid the problem of varying land-sea masks that arise due to the different native grids and the regridding process. For 19 out of the 33 investigated models, the land-ice fraction variable (sftgif) is available. We find an average land-ice cover of 77% with a minimum value of 63% and a maximum value of 85% for our masked region.

We obtain spatiotemporally resolved as well as scalar scaling factors for the near-surface temperatures and precipitations against the global mean temperature (GMT) and time. For the scalar scaling factors, we use a linear fit of the spatially weighted annual and seasonal (winter and summer) near-surface temperatures and precipitation rates in Greenland against the respective

https://doi.org/10.5194/egusphere-2024-1597
Preprint. Discussion started: 27 June 2024

model GMTs. For the precipitation we follow a similar approach to Nicola et al. (2023) and fit the log-scaled precipitation against the respective temperatures, motivated by the Clausius–Clapeyron relationship. We define the sensitivity of precipitation for each degree of warming s as

$$s = 100\frac{\%}{\mathrm{K}} \cdot (e^{k/\mathrm{K}} - 1), \tag{3}$$

where k/K is the unitless growth factor from Equation 1. This follows from the assumption that the precipitation P increases exponentially with the sensitivity s according to

$$P = P_0 \left(1 + \frac{s}{100\%/\mathrm{K}}\right)^{\Delta T/\mathrm{K}} \tag{4}$$

for a temperature change ΔT. Then a linear regression of $\ln(P)$ against T directly gives k as a fit parameter and s can be calculated according to Equation 3. It has to be noted that k is sometimes directly defined as the precipitation sensitivity (Held and Soden, 2006; Nicola et al., 2023). However, for small $k < 0.1$, $k \approx s$ and they can easily be converted between one another.

For the spatial scaling factors, we fit the local near-surface temperatures and precipitations, that is, every grid cell against the GMT. Additionally, we derive scaling factors of the local precipitation against local near-surface temperature (Fig. I1).

We force the ice sheet model PISM with the CMIP6 outputs to show the difference in the short- and long-term behaviour of the GrIS for spatiotemporal anomalies and for spatially uniform anomalies. For the short-term model forcing, we use the average near-surface temperature and precipitation anomalies for each scenario compared to the time period 1980-2000. First, we calculate the CMIP6 ensemble average fields for each scenario and the historical time period 1980-2000. We calculate the monthly anomalies by subtracting the historical climatology from the ensemble averages until the year 2100. Subsequently, we regrid the average anomalies to the 20 km PISM grid using a first-order conservative algorithm (nco) (Zender, 2008). Additionally, we smooth the obtained regridded fields using cdo smooth (Schulzweida, 2023) with a smoothing radius of 40 km to avoid artefacts stemming from the interpolation. Thereby, we obtain spatially resolved monthly anomaly fields of the precipitation and near-surface temperature from 2015 to 2100. For the scalar forcing, we calculate the spatially weighted means of the regridded and smoothed monthly near-surface temperature and precipitation anomaly fields that we used for the spatial forcing. For the long-term model forcing, we calculate the 10 year average of the monthly near-surface temperature and precipitation anomalies from 2090-2100.

2.2 PISM

We use the Parallel ice sheet model (PISM) in the version v2.1-1-g6902d5502 (Winkelmann et al., 2011) with the dEBM-simple surface mass balance module (Krebs-Kanzow et al., 2018, 2021; Zeitz et al., 2021). This model configuration has successfully been used for future projections of the GrIS before (Zeitz et al., 2021; Bochow et al., 2023) and has been shown to realistically reproduce past ice sheet states (Zeitz et al., 2021; Garbe et al., 2023). We mostly follow the ice sheet initialisation and setup from Bochow et al. (2023).

PISM is a thermomechanically coupled ice sheet model using the shallow-shelf (SSA) and shallow-ice approximation (SIA). The ice rheology is based on the Glen–Paterson–Budd–Lliboutry–Duval flow law (Lliboutry and Duval, 1985) with an exponent

https://doi.org/10.5194/egusphere-2024-1597
Preprint. Discussion started: 27 June 2024

of $n = 3$ and the enhancement factors $E_{\mathrm{SIA}} = 3$ and $E_{\mathrm{SSA}} = 1$. Furthermore, we use a pseudo-plastic sliding law (Schoof and Hindmarsh, 2010) with the exponent factor $q = 0.5$. We use the Lingle-Clark Earth deformation model with a lithosphere flexural rigidity of $5 \cdot 10^{24}$ Nm, mantle density of 3300 kg/m^3 and a mantle viscosity of $1 \cdot 10^{24}$ Pas. We apply a spatially uniform lapse rate of 6 K/km across the whole ice sheet. The precipitation scales with the surface-height-induced near-surface temperature change by a factor of 5.5 %/K. We prescribe a front-retreat calving based on the observed present-day extent of the GrIS. For the dEBM-simple melt equation Zeitz et al. (2021), we use the parameters $c_1 = -90\,\mathrm{W/m^2K}$ and $c_2 = 30\,\mathrm{W/m^2}$. The orbital parameters do not vary and are fixed to present-day values.

We spinup the ice sheet to a close to present-day state by bootstrapping the model from present-day conditions, including ice thickness, bedrock elevation (Morlighem et al., 2017) and basal heat flux (Shapiro and Ritzwoller, 2004) and letting it reach equilibrium. We force the model with the climatological mean near-surface temperature and precipitation fields from the years 1980-2000 from the regional climate model MARv3.12 (Fettweis et al., 2017). We run the model for at least 100,000 years to reach an equilibrium ice sheet state. We use a horizontal resolution of 20 km and a vertical resolution of 40 m.

3 Greenlands climate in CMIP6

3.1 Temperature projections in CMIP6

Due to Arctic amplification, Greenland's near-surface temperatures have increased faster than the GMT; this enhanced warming is expected to continue in the future (Serreze and Barry, 2011; Rantanen et al., 2022; Preece et al., 2023). Arctic amplification is the process of accelerated warming in the high latitudes compared to lower latitude because of several feedback mechanisms, most prominently the ice-albedo feedback (Screen and Simmonds, 2010) and the lapse-rate feedback (Stuecker et al., 2018). However, the future extent of Arctic amplification remains uncertain and and previous studies report an Arctic warming up to 4 times faster than the global average (Rantanen et al., 2022).

The projected rise in the GMT in CMIP6 is generally higher than in the previous model intercomparison CMIP5 (Tebaldi et al., 2021). For Greenland, most CMIP6 models have a higher near-surface temperature sensitivity than the corresponding CMIP5 models (Zhang et al., 2024). The near-surface temperatures in Greenland are relatively constant in all models until the year 1980 (Fig. 1a). However, there is an accelerated rise in the near-surface temperatures between 1980 and 2100. Only the most optimistic SSP1-2.6 scenario shows a relatively constant near-surface temperature in Greenland after 2050. We find an ensemble mean model near-surface temperature rise in Greenland of $\Delta T = 3.27 \pm 1.50$°C (SSP1-2.6), 4.98 ± 1.75°C (SSP2-4.5), 6.73 ± 2.06°C (SSP3-7.0) and 8.15 ± 2.30°C (SSP5-8.5) above pre-industrial (1850-1900) level by 2090-2100 (Fig. 1a). There is a considerable spread in the model response with one model even predicting a near-surface temperature decrease by 2100 under the SSP1-2.6 scenario (Fig. 1a).

In all scenarios, the ensemble mean of the annual mean near-surface temperature responds in good approximation linearly to the increase in the GMT (Fig. 2a). We find a scaling factor ranging from $s = 1.29$ (SSP1-2.6) to $s = 1.54$ (SSP3-7.0) of the annual regional near-surface temperature against the GMT until 2100 (Fig. 2a), suggesting a state-dependence of the scaling factor. The scaling factor or sensitivity can be interpreted as a Greenland specific amplification factor analogously to

https://doi.org/10.5194/egusphere-2024-1597
Preprint. Discussion started: 27 June 2024

the Arctic amplification. While the annual near-surface temperature in the historical period also shows a linear response, it shows a stronger warming of Greenland with $s = 2.0$ compared to the future scenarios. The warming is generally stronger in the winter season (DJF) with more than 40% faster warming than in the summer (JJA) for all future scenarios, except SSP1-2.6 (Fig. 2b,c). In the SSP1-2.6 scenario, the warming in winter and summer shows the same response with $s = 1.16$. However, the winter temperatures in SSP1-2.6 do not follow a strong linear trend ($R^2 = 0.46$). In the historical period, the winter temperatures increase more than 50% faster than the summer temperatures. This is less than some previously reported values which indicated twice as much warming in winter than in summer (Robinson et al., 2012).

There is a considerable inter-model spread in the spatially averaged scaling factors (Fig. A1). Specifically, the SSP1-2.6 scenario shows a large inter-model spread, ranging from 0 to 2.25 in the summer and from -2 to 4 in the winter (Fig. A1a,b). In other words, in some models the spatially averaged winter near-surface temperature in Greenland decreases two times faster than the GMT increases, while in other models the near-surface temperature increases 4 times faster than the GMT. In general, the spread in the response of the winter temperatures is larger than in the summer and annual temperatures (Fig. A1b). Furthermore, the more extreme the future scenario, the smaller the range in the scaling factors, besides the annual temperatures in the SSP2-4.5 scenario. The historical runs show the highest scaling factors for summer, winter and annual temperatures. Additionally, we show the relationship between the winter and summer temperatures.

In all future scenarios, besides SSP1-2.6, the majority of the models show a faster increase of the winter temperatures than the summer temperatures, i.e. $s > 1$ (Fig. A1d). However, the uncertainty is considerable. The ensemble mean of the spatially-averaged scaling factors agrees with the scaling factors derived from the ensemble mean of the near-surface temperatures. This suggests that the response of the ensemble mean temperatures is an adequate representation of the mean scaling factors. It also has to be noted that the relationship between the GMT and the spatially averaged seasonal temperatures for some models does not necessarily follow a clear linear relationship. This is especially visible when comparing the scaling factors for each season against the GMT and the scaling factors of the individual seasons against each other (Fig. A1d).

There is a clear spatial dependency of the temperature sensitivity in Greenland (Fig. 2d-g). Generally, there is a north-south gradient in the ensemble mean annual near-surface temperature with decreasing temperature sensitivity towards the South in all scenarios. For SSP1-2.6, all of Greenland approximately south of the Ilulissatfjord shows a sensitivity below 100%, that is, it warms slower than the GMT. This 100%-contour migrates southward the more extreme the scenario (Fig. 2d-g). For the SSP3-7.0 and the SSP5-8.5 scenario, only the southernmost part of Greenland shows a slower mean annual warming than the global mean (Fig. 2g) However, there is a pronounced seasonal difference in the spatial response. While the summer temperatures increase faster in the interior of the GrIS than at the margins, the winter temperatures show a north-south gradient with considerably more warming in the northern parts of the ice sheet (Fig. C1). While this spatial dependence varies in intensity between the scenarios, it is consistent across all future scenarios.

For the historical period, there is rather a clear warming gradient between the interior and the margin of the GrIS than a gradient between north and south (Fig. C1a). However, this gradient is inverted in summer compared to winter (Fig. C1f). In winter, the margins of the ice sheet warm considerably faster than the interior, with a scaling factor exceeding 300% at the margin and less than 200-250% in the interior of the GrIS. On the other hand, in the summer most of the interior ice sheet

https://doi.org/10.5194/egusphere-2024-1597
Preprint. Discussion started: 27 June 2024

warms up to 150% faster than the global average, with a decrease of the scaling factor toward the margin. The gradient in summer is not as pronounced as in winter. These sensitivities are in accordance with observational temperature records in southwestern Greenland, which show a 2.4 times stronger warming in the winter than in the summer for the time period 1850-2019 (Cappelen, 2020; Bochow et al., 2023). In both seasons, almost entire Greenland shows stronger warming in the historical period than in the future scenarios.

The inter-model spread in the spatial response is relatively large. Here, we only show the spatial differences for the annual temperatures but similar pictures arise for the individual seasons. Especially for the most optimistic SSP1-2.6 scenario, there is a pronounced difference in the different model responses (Fig. E1). Several models show a near-surface temperature decrease for the 21st century, mostly in the southern and southwestern parts of Greenland. The two models CESM2 and CESM2-WACCM even project a near-surface temperature decrease for most of Greenland except for the northernmost part. This is mostly due to a strong decrease of the winter temperatures in these models. For the SSP2-4.5 scenario, a minority of models show a decrease of the temperatures at the southwestern margins (Fig. F1). In the SSP3-7.0 scenario, only one model (FGOALS-g3) shows a decrease of the annual temperatures at the southern margin (Fig. G1). Similarly, only the FGOALS-g3 model shows a minimal near-surface temperature decrease at the southernmost margin in the SSP5-8.5 scenario (Fig. H1). In general, the more extreme the scenario, the more uniform the model responses become.

For the historical runs, all models show a clear increase of the mean annual temperatures in all of Greenland (Fig. D1). However, similar to the future scenarios, there are clear differences in the magnitude of temperature change (relative to the model GMT). The EC-Earth3-Veg-LR model shows the strongest response out of all models, with a temperature sensitivity of more than 300% in most of Greenland. In contrast, several models such as NorESM2-LM show a slower warming than the GMT, i.e. a scaling factor smaller than 100%, in some parts of Greenland.

The regional ensemble mean temperatures show a relatively strong linear dependence on the GMT in all scenarios and seasons, with a mean $R^2 > 0.7$ (Fig. C1,2&B1). Only the winter temperatures in the SSP1-2.6 scenario (Fig. C1b) show a relatively small coefficient of determination $R^2 = 0.36$. The R^2 values show the lowest values in southwestern Greenland (Fig. B1a) with a steady increase towards the north. However, this spatial dependence is only pronounced for the low emission scenarios. The linear relationship between the regional temperatures and the GMT is also clearly visible in the single model regional scaling factors, especially for the SSP3-7.0 and SSP5-8.5 scenarios, where $R^2 > 0.7$ for most models (Fig. D1-H1).

3.2 Precipitation projections in CMIP6

Similar to the near-surface temperature projections, the precipitation rates in Greenland are expected to increase in the future, with a stronger response in CMIP6 than in CMIP5 (Zhang et al., 2024). Similar to the near-surface temperature anomalies, the precipitation anomalies stay relatively constant until 1980. In all scenarios, we find an increase of the ensemble mean annual precipitation rates compared to the reference period 1850-1900 (Fig. 1b). However, some models in the SSP1-2.6 and SSP2-4.5 scenarios predict a decrease of the annual precipitation rates at the end of the 21st century. We find an ensemble mean of the annual precipitation increase of $\Delta P = (804 \pm 633)$ mm/year (SSP1-2.6), 1302 ± 715 mm/year (SSP2-4.5), 1866 ± 954 mm/year (SSP3-7.0) and 2326 ± 1093 mm/year (SSP5-8.5) by the year 2090-2100 (Fig. 1b). While the ensemble mean precipitation

https://doi.org/10.5194/egusphere-2024-1597
Preprint. Discussion started: 27 June 2024

anomalies show a similar response as the temperature anomalies, the uncertainty, or ensemble spread, is larger than for the temperatures.

The log of the ensemble mean annual precipitation shows an increase in all scenarios, including the historical period (Fig. 3a). The highest precipitation sensitivity is observed in the historical period with $s = 8.35\%$/K, followed by the SSP5-8.5 scenario with $s = 6.09\%$/K, SSP3-7.0 with $s = 5.53\%$/K, SSP2-4.5 with $s = 3.74\%$/K and SSP1-2.6 with $s = 3.02\%$/K. However, the relationship between log precipitation and GMT is not necessarily clearly linear, i.e. the precipitation rates do not necessarily increase exponentially with the GMT. Specifically, for the SSP1-2.6 scenario, the coefficient of determination is only $R^2 = 0.27$, and for the historical period $R^2 = 0.58$. This might be a consequence of the small increase in the GMT in these two scenarios, leading to a larger contribution of the interannual precipitation variability to the observed precipitation changes. For the more extreme scenarios (SSP3-7.0 and SSP5-8.5), the linear relationship between log precipitation and GMT is very clear ($R^2 > 0.9$).

A similar picture arises for the ensemble means of the summer and winter precipitation changes (Fig. 3b,c). The sensitivity of the summer precipitation is higher in all future scenarios and more uniform across all scenarios than the winter sensitivity, ranging from $s = 4.6\,\%$/K in the SSP2-4.5 scenario to $s = 7.03\,\%$/K in the SSP5-8.5 scenario (Fig. 3b). We find a winter precipitation sensitivity of $-2.79\,\%$/K (SSP1-2.6), $2.82\,\%$/K (SSP2-4.5), $4.37\,\%$/K (SSP3-7.0), $4.61\,\%$/K (SSP5-8.5) and $11.30\,\%$/K for the historical time period. This implies a reduction of winter precipitation rates with increasing GMT for the SSP1-2.6 scenario. However, similarly to the changes in the annual precipitation anomalies, the historical, SSP1-2.6 and partially the SSP2-4.5 precipitation sensitivities show a small coefficient of determination for seasonal precipitations (Fig. 3b,c). Additionally, the inter-model spread is considerable, especially for the winter precipitation sensitivity (Fig. K1c). For example, for the SSP1-2.6 scenario, the standard deviation of the winter precipitation sensitivity is considerably larger than the sensitivity itself. The SSP1-2.6 winter precipitation sensitivity ranges from -29%/K for the NorESM2-LM model to 26%/K for the BCC-CSM2-MR model. It also has to be noted that the R^2-coefficient of the spatially averaged precipitation sensitivity is very small for most fits, i.e. $R^2 < 0.1$, especially for the moderate scenarios. This indicates that a spatially and seasonally uniform precipitation sensitivity for the whole GrIS is not an appropriate modelling choice.

This is further supported by the spatial patterns of the ensemble mean of the annual precipitation sensitivities (Fig. 3d-g). In all scenarios, there is a clear northeast-southwest gradient in the sensitivity. The northeastern part of Greenland shows the highest annual precipitation increase with increasing GMT in all scenarios. Interestingly, the spatial sensitivity differences are largest in the SSP1-2.6 scenario with $s > 15\,\%$/K in the northeast of Greenland to $s < 0\,\%$/K at the southern and southeastern margin (Fig. 3d). In the SSP2-4.5 scenario, only the southernmost tip of Greenland shows a negative precipitation sensitivity (Fig. 3e). In all other scenarios, the annual precipitation sensitivity is positive, i.e. there is an increase of the precipitation with an increase of the GMT in all of Greenland. The seasonal difference in the spatial responses is relatively pronounced (Fig. J1). In winter (Fig. J1a-e), the precipitation increase is most pronounced in northern Greenland, with less precipitation increase in western and southeastern Greenland. For the SSP1-2.6 scenario, large parts of southern Greenland show a negative precipitation sensitivity. In summer (Fig. J1f-j), eastern Greenland shows the highest sensitivity. In the historical period, the spatial sensitivity patterns are relatively similar to the other scenarios (Fig. J1a,f). However, western and northeastern Greenland show a slightly

https://doi.org/10.5194/egusphere-2024-1597
Preprint. Discussion started: 27 June 2024

lower precipitation sensitivity in the historical period for both winter and summer than the future scenarios (Fig. J1). At the same time, the winter precipitation sensitivity of southeastern Greenland is substantially higher for the historical period. While we show sensitivities of the ensemble mean precipitation rates, the ensemble mean of the single-model sensitivities show similar patterns and intensities.

Interestingly, the R^2-values of the fit of the ensemble mean precipitation rates against GMT are relatively low for the moderate emission scenarios (Fig. B1e,f & J1). At the margins and especially at the southeastern margin, the R^2-values are small due to high precipitation variability in these regions (Fig. B1e-h). Similarly, the R^2-values of the single model precipitation sensitivities are very low for most models in all scenarios, i.e. $R^2 < 0.2$, indicating that there is not a clear linear relationship between $\ln(P)$ and the GMT or mean temperatures in Greenland in individual models (Fig. L1-P1). However, for the SSP3-7.0 and SSP5-8.5 scenario, the log ensemble mean annual precipitation rates show a clear linear relationship with the GMT ($R^2 > 0.77$) (Fig. B1g,h).

Since the spatially averaged annual and seasonal temperatures in Greenland show a strong linear relationship with the GMT (Fig. 2a-c), the precipitation sensitivities relative to the GMT can easily be converted to precipitation sensitivities relative to the spatially averaged regional Greenland near-surface temperatures. The resulting sensitivities are slightly lower due to the accelerated increase of near-surface temperatures in Greenland compared to the GMT, but do not show a substantial change in the spatial patterns (Fig. I1).

The inter-model spread in the spatial response is large for the summer precipitation and for the winter precipitation in all scenarios. Several models show strong variation from the cross-model mean of the summer precipitation sensitivity, with predicted precipitation decreases in large parts of Greenland, especially for the moderate scenarios. This is also visible in the annual precipitation sensitivities (Fig. L1-P1). The spatial response differs wildly between the single models, especially for the SSP1-2.6 scenario (Fig. M1).

4 Modelling the response of the ice sheet

To show the influence of the modelling choices, we run simulations with the ice sheet model PISM-dEBM-simple with spatially resolved and spatially uniform scaling factors for all analysed SSP scenarios.

4.1 Short-term response

We initialise the ice sheet to a close to present-day state corresponding to the year 2015. Subsequently, we run the model with the dEBM-simple surface mass balance module (Zeitz et al., 2021), which only needs precipitation and temperatures as input until the year 2100. We keep the orbital parameters fixed in all runs to exclusively extract the influence of the sensitivity choices.

There is a clear difference in the ice sheet volume after 85 years (Fig. 4a). The runs begin to branch after approximately 15 to 20 years. In each case, the simulations with a spatially uniform scaling factor (dashed lines in Fig. 4a) show a smaller

https://doi.org/10.5194/egusphere-2024-1597
Preprint. Discussion started: 27 June 2024

ice volume than the corresponding simulations with spatially resolved scaling factors. The difference is more pronounced the more extreme the scenario.

The spatial differences show the same pattern for each scenario (Fig. 4b-e). The ice sheet thickness is generally smaller at the southwestern margin when the model is forced with the scalar anomalies (blue in Fig. 4b-e). In contrast, the ice thickness at the southeastern margin, and partially in the interior of Greenland, is larger for the simulations with scalar anomalies for each scenario (red). These differences are more pronounced the more extreme the scenario. For the moderate scenarios SSP1-2.6 and SSP2-4.5, the difference in the ice thickness after 85 years is in the magnitude of 10 m to 20 m (Fig. 4b,c). For the SSP5-8.5 scenario, the ice thickness difference is more than 40 m at the southeastern and southwestern margins and partially extending further into the ice sheet.

This observed influence of the scaling factors is in accordance with the spatial sensitivities shown before. The southwestern margin of the GrIS shows a smaller near-surface temperature increase than the average GrIS, especially for the annual melt period (summer) (Fig. C1f-j). This leads to an overestimated melt rate in this region for the scalar temperature anomalies. In contrast, the precipitation sensitivity at the southwestern margin is relatively close to the GrIS-wide average (Fig. J1). Similarly, the temperature-driven melt is larger for the spatially resolved anomalies at the northern ice sheet margins. For the southeastern margin, the changes in the simulated ice sheet thickness are mostly due to the differences in the precipitation sensitivities. The precipitation increase per degree of warming is smaller at the southeastern margin than the GrIS-wide average (Fig. 3d-g). In the SSP1-2.6 scenario, there is even a decrease of the precipitation rates. This leads to less accumulation and hence reduced SMB in this region compared to the uniform scaling factors. In fact, the spatial patterns of the precipitation sensitivity agree very well with the ice thickness difference in eastern Greenland observed by the year 2100.

4.2 Long-term response

We extend the short-term simulations for another 100,000 years with temporally constant monthly near-surface temperature and precipitation anomalies, derived from the average 2090-2100 CMIP6 climatologies.

The long-term response of the ice sheet varies substantially between spatially resolved and uniform scaling factors (Fig. 5 & 6). Similar to the short-term response, the ice volume is generally smaller for scalar near-surface temperature and precipitation anomalies than for spatially resolved anomalies (Fig. 5). The difference is most pronounced for the SSP2-4.5 scenario. In this scenario, the ice sheet is completely lost temporarily with scalar anomalies. In contrast, for the spatially resolved anomalies, the ice sheet recovers to 50% of its initial volume after first reaching approximately 30% of its initial volume. Also for the scalar anomalies, the ice sheet shows a temporary rebound to 50% of its initial volume after circa 70,000 years after the complete loss. However, the ice volume decreases equally fast as it recovers in this case.

For the SSP1-2.6 scenario, the ice sheet response between spatially resolved and uniform anomalies is very similar. The ice sheet loss is limited to 15-20% of the initial ice sheet volume in both cases. While the simulations with scalar anomalies generally show a 5-10% smaller ice volume than the corresponding simulations with spatial anomalies, both simulations show oscillations of the ice sheet on decamillennial time scales. These quasi-periodic decamillennial oscillations of the ice sheet have been observed before and are believed to be a nonlinear interplay between the glacial isostatic adjustment (GIA) and

https://doi.org/10.5194/egusphere-2024-1597
Preprint. Discussion started: 27 June 2024

the melt elevation feedback (Zeitz et al., 2022; Bochow et al., 2023; Petrini et al., 2023). The reduced ice sheet volume due to increased surface temperatures leads to less load on the bedrock below the ice sheet. Subsequently, the bedrock lifts up and leads to decreasing temperatures at the ice surface, enabling partial regrowth of the ice sheet, which in turn depresses the bedrock again, closing the feedback loop.

For the SSP3-7.0 and SSP5-8.5 scenarios, the ice sheet is lost almost completely without any recovery, independently of choosing spatially resolved or uniform scaling factors. However, the time scale of the loss differs between the scalar and spatially resolved anomalies. For the SSP3-7.0 scenario, the ice sheet is completely lost (ice volume below $0.25 \cdot 10^{15}\,\mathrm{m}^3$) after 11,400 years (spatially resolved anomalies) and after 5,200 years (scalar anomalies), respectively. Similarly, the ice sheet is lost after 4,900 years (spatially resolved anomalies) and after 2,900 years (scalar anomalies), respectively, in the SSP5-8.5 scenario.

The spatial evolution of the ice sheet shows similar patterns for spatially resolved and uniform scaling factors (Fig. 6). However, there are differences in the time scale and extent of the ice sheet retreat. For the spatially resolved anomalies, the southwestern part of the ice sheet is most sensitive to warming, followed by a gradual retreat from the south to the north of the GrIS with a rather abrupt loss of the remaining northern part. In the SSP2-4.5 scenario with spatially varying anomalies, the southeastern part regrows simultaneously with the loss of the remaining northern part of the GrIS, which is also visible in the minimum extent during the 100,000 years of simulation (red line in Fig. 6b). This leads to the observed quasi-oscillatory behaviour in the ice volume (Fig. 5). Similarly, the southwestern GrIS is most sensitive to warming in the case of scalar anomalies. However, in contrast to spatially resolved anomalies, the northern part retreats almost simultaneously with the southern part of the GrIS.

For the SSP1-2.6, SSP3-7.0 and SSP5-8.5 scenarios, the spatial extent of the ice sheet after 100,000 years is similar for scalar and spatially resolved anomalies (Fig. 6). Furthermore, the minimum extent during the whole simulation is very similar between spatially resolved and uniform scaling factors. Only the SSP2-4.5 scenario shows a very different minimum extent and extent at the end of the simulation (Fig. 6b,f), which is also visible in the ice volume (Fig. 5). The interplay between GIA and melt-elevation feedback becomes more important close to the critical temperature threshold beyond which the ice sheet melts completely. While the surface temperatures are high enough to melt large parts of the ice sheet, the subsequent bedrock rebound still allows partial regrowth of the ice sheet. The SSP2-4.5 anomalies are close to this threshold, therefore the difference between the scalar and spatially resolved near-surface temperature and precipitation anomalies is especially pronounced. In contrast, for the SSP3-7.0 and SSP5-8.5 scenario, the GIA does not allow a regrowth anymore.

5 Conclusions

We analysed the precipitation and near-surface temperature changes in Greenland for the time period from the year 1850 until the year 2100 based on the output of the latest coupled model intercomparison project (CMIP6). We find a temperature sensitivity between $s = 1.29$ (SSP1-2.6) and $s = 1.53$ (SSP5-8.5) between annual mean temperatures in Greenland and the GMT. Additionally, we find a sensitivity of the mean annual precipitation rates between $s = 3.02\,\%/\mathrm{K}$ and $s = 6.09\,\%/\mathrm{K}$,

https://doi.org/10.5194/egusphere-2024-1597
Preprint. Discussion started: 27 June 2024

compared to the GMT. We find a clear seasonal dependency, both for the temperature scaling and the precipitation sensitivities. Our precipitation sensitivities are below the theoretically derived value from the Clausius-Clapeyron relationship of 9%/K, in accordance with other studies (Robinson et al., 2012; Frieler et al., 2012, 2015; Nicola et al., 2023; Bochow et al., 2023). Our temperature scaling factors are in accordance with an earlier study, which only investigated temperature scaling factors for the historical and SSP5-8.5 scenarios (Bochow et al., 2023). At the same time, our summer temperature scaling factors are higher for all scenarios than a previous estimate based on CMIP3, which estimated a scaling factor of $s = 0.9 \pm 0.2$ between summer near-surface temperature in Greenland and the GMT (Robinson et al., 2012). Similarly, our winter temperature scaling factors are lower than reported by Robinson et al. (2012). Robinson et al. (2012) report a 2.1 times faster warming in winter compared to the summer, while we only find a ca. 1.4 times faster warming during the winter than during the summer. These differences are very likely due to the substantial changes in the climate models between CMIP3 and CMIP6.

The differences in the precipitation sensitivities between the different emission scenarios and the historical period can be interpreted as a state-dependency of the precipitation sensitivities, that is, the sensitivity is dependent on the background climate and not only on the regional temperatures. We attribute this to other global warming induced changes such as changes in dynamic processes that strongly influence precipitation patterns and rates in Greenland (Mernild et al., 2015; Auger et al., 2017; Lewis et al., 2017, 2019). While our approach takes all changes in the precipitation rates into account, we do not distinguish between thermodynamic and dynamically induced changes in the precipitation rates. In other words, our approach assumes that all changes in the precipitation rates are a direct consequence of temperature change. The low R^2 values for individual model fits supports the conclusion that the changes in precipitation are not necessarily driven by temperature changes alone, but rather by warming-induced changes in, for example, atmospheric circulations. Especially for the moderate emission scenarios, the low R^2 values are a consequence of strong precipitation variability for low levels of warming. It has been shown that the North Atlantic Oscillation, Atlantic Multidecadal Oscillation and the Icelandic low have significant correlation with observational precipitation rates across Greenland (Mernild et al., 2015; Auger et al., 2017). Specifically, the eastern margin of Greenland shows a high precipitation variability in CMIP6 and observations, which has been linked to the North Atlantic storm track (Groves and Francis, 2002; Bogerd et al., 2020). Auger et al. (2017) conclude that increased blocking events in a warmer climate would lead to an increase of variability and likelihood of precipitation in southwest in Greenland and to the opposite effect in southeast Greenland. While this does not directly translate to precipitation sensitivities, we find a generally lower or even negative precipitation sensitivity in southeastern compared to southwestern Greenland (Fig. 3d-g). However, the representation of such atmospheric changes in the current generation of climate models is not clear (Delhasse et al., 2021). The observed state dependency of the sensitivities also implies that historical changes might not be an appropriate predictor for future changes. For example, the average regional temperatures in Greenland show a higher scaling with the GMT than all future scenarios, even though the linear relationship holds across all scenarios. Scaling factors or sensitivities solely derived from historical data might over- or underestimate future responses. Nevertheless, ideally, observational data should be included for parameterisations to complement modelling results.

Given the strong differences in model responses, the use of a limited selection of climate models or even of individual models to estimate precipitation or temperature changes can lead to vastly different values. Similarly, using single climate

https://doi.org/10.5194/egusphere-2024-1597
Preprint. Discussion started: 27 June 2024

model runs as forcing for standalone ice sheet modelling can produce very different outcomes. We therefore argue that the use of single model runs as forcing for ice sheet modelling, especially on long time scales, needs to be treated with caution. We either suggest the use of (i) ensemble mean climate fields as forcing, which minimise the influence of short-term climate variability on the ice sheet, or (ii) ensemble simulations with single model forcing fields. Additionally, the second option allows, in principle, a statistical treatment of the different outcomes. However, running ensemble simulations with different forcing is computationally substantially more expensive.

Interestingly, the average regional warming in Greenland by the year 2100, as predicted by the CMIP6 models, is close or even above the critical temperature threshold of the GrIS, which has been estimated between $0.8°C$ and $3.0°C$ GMT relative to pre-industrial levels (Armstrong McKay et al., 2022). Even for the SSP1-2.6 scenario, the ensemble mean regional warming in Greenland for 2090-2100 is $\Delta T = 3.27°C$ above pre-industrial levels (Fig. 1a), which translates to a global warming level of $\Delta T_{\text{GMT}} = 2.5°C$ using the corresponding scaling factor for the SSP1-2.6 scenario of $s = 1.29$ (Fig. 2a). Hence, the critical temperature threshold for the Greenland ice sheet might be crossed, at least temporarily, even in the optimistic emission scenarios. However, it has been shown that a temporary overshoot of the critical threshold for the GrIS does not necessarily imply a large-scale loss of the ice sheet (Bochow et al., 2023; Höning et al., 2024).

We show that scalar near-surface temperature and precipitation anomalies, that are often used for long-term modelling of ice sheets, can lead to over- or underestimation of the accumulation and ablation rates and hence the surface mass balance. For the Greenland ice sheet, simulations with scalar near-surface temperature anomalies based on a Greenland-wide average might overestimate melt rates in large parts of the GrIS. On the other hand, spatially and seasonally uniform precipitation sensitivities might lead to an overestimation of accumulation rates in southern Greenland and an underestimation in northern Greenland. The difference between spatially varying and uniform scaling factors is already clearly visible in short-term simulations but has an even bigger influence on long-term simulations. Ultimately, spatially uniform sensitivities and anomalies in simulations might lead to an underestimation of the long-term stability of parts or even the whole GrIS. Similar concerns have been raised about scalar lapse rates which are often used in ice sheet modelling (Crow et al., 2024). It is known that the lapse rate in Greenland has a seasonal and spatial dependency (Erokhina et al., 2017) and it has been shown that using spatially and temporally varying lapse rates has a substantial influence on the ice sheet evolution (Crow et al., 2024).

While we have shown that spatially uniform anomalies capture the overall evolution of the GrIS, they tend to over- or underestimate the surface mass balance of parts of the ice sheet. They therefore lead to over- or underestimated projections of sea level or long-term stability of the GrIS. Since fully coupled simulations on long time scales will most likely not be feasible in the near future, we recommend the use of spatially and monthly resolved anomalies for long-term ice sheet modelling instead of spatially uniform anomalies.

https://doi.org/10.5194/egusphere-2024-1597
Preprint. Discussion started: 27 June 2024

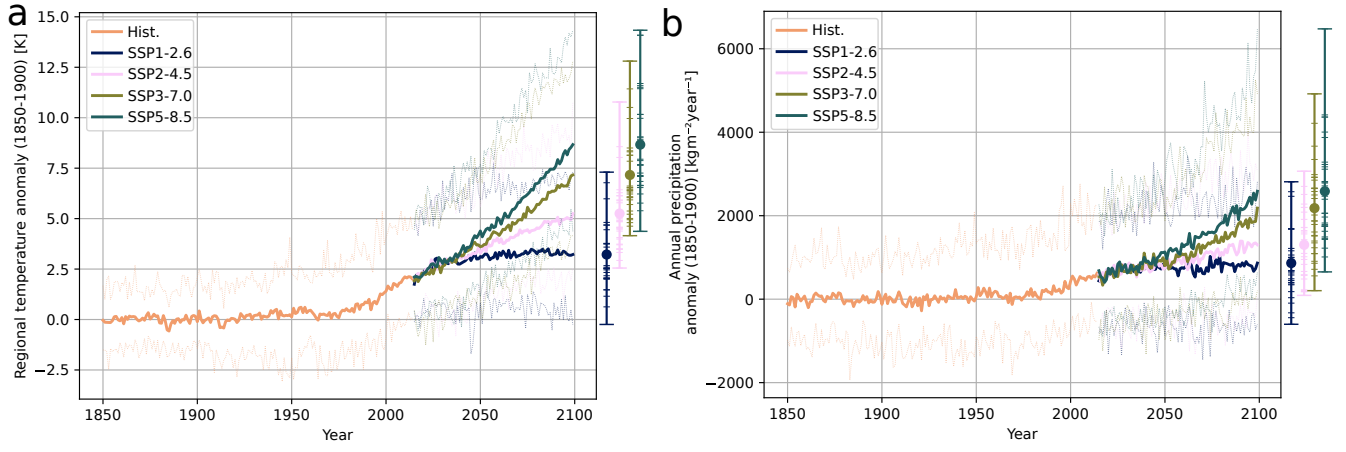

Figure 1. Ensemble mean of Greenland mean annual near-surface temperature and precipitation anomalies in CMIP6 relative to pre-industrial levels. (a) Ensemble mean of annual near-surface temperature anomalies as predicted by CMIP6 models for all SSP scenarios relative to pre-industrial level (1850-1900). The solid lines denote the ensemble mean, while the dashed lines denote the minimum and maximum anomalies for the respective scenario. The horizontal lines on the bar denote the end-value in the year 2100 for each model, while the dot is the mean of the near-surface temperature in the year 2100. **(b)** Same as **a** but for the annual precipitation. In each scenario, the ensemble mean of the near-surface temperature and precipitation increase.

https://doi.org/10.5194/egusphere-2024-1597
Preprint. Discussion started: 27 June 2024

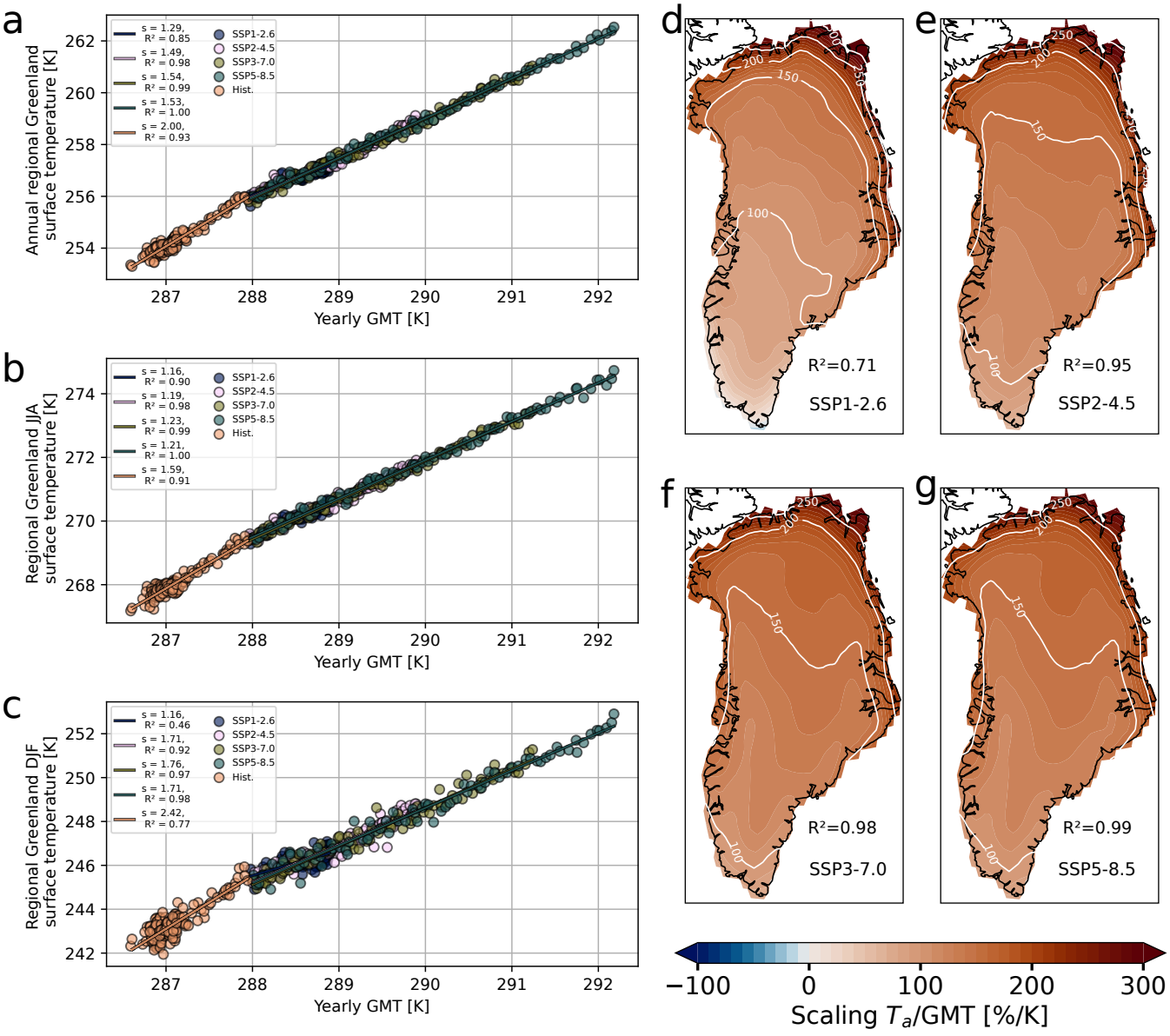

Figure 2. Ensemble mean and spatial scaling factors for near-surface temperatures relative to global mean temperatures. (a) Fit of the ensemble mean of the annual regional near-surface temperature in Greenland against the ensemble mean GMT for all SSP scenarios and the historical time period. **(b,c,)** Same as **a** but for the summer (JJA) and winter (DJF) temperatures in Greenland, respectively. The DJF temperatures generally increase faster than the JJA temperatures for all scenarios except for SSP1-2.6. **(d)** Regional scaling factors for ensemble mean of annual surface temperatures in Greenland against GMT for SSP1-2.6. The contour at 100% denotes the area where the regional near-surface temperature increases faster than the GMT. **(e, f, g)** Same as **d** but for SSP2-4.5, SSP3-7.0 and SSP5-8.5, respectively. In all scenarios, northern Greenland warms fastest compared to the GMT with a gradient towards to the South. The Southern tip of the GrIS warms slower than the GMT in each scenario.

https://doi.org/10.5194/egusphere-2024-1597
Preprint. Discussion started: 27 June 2024

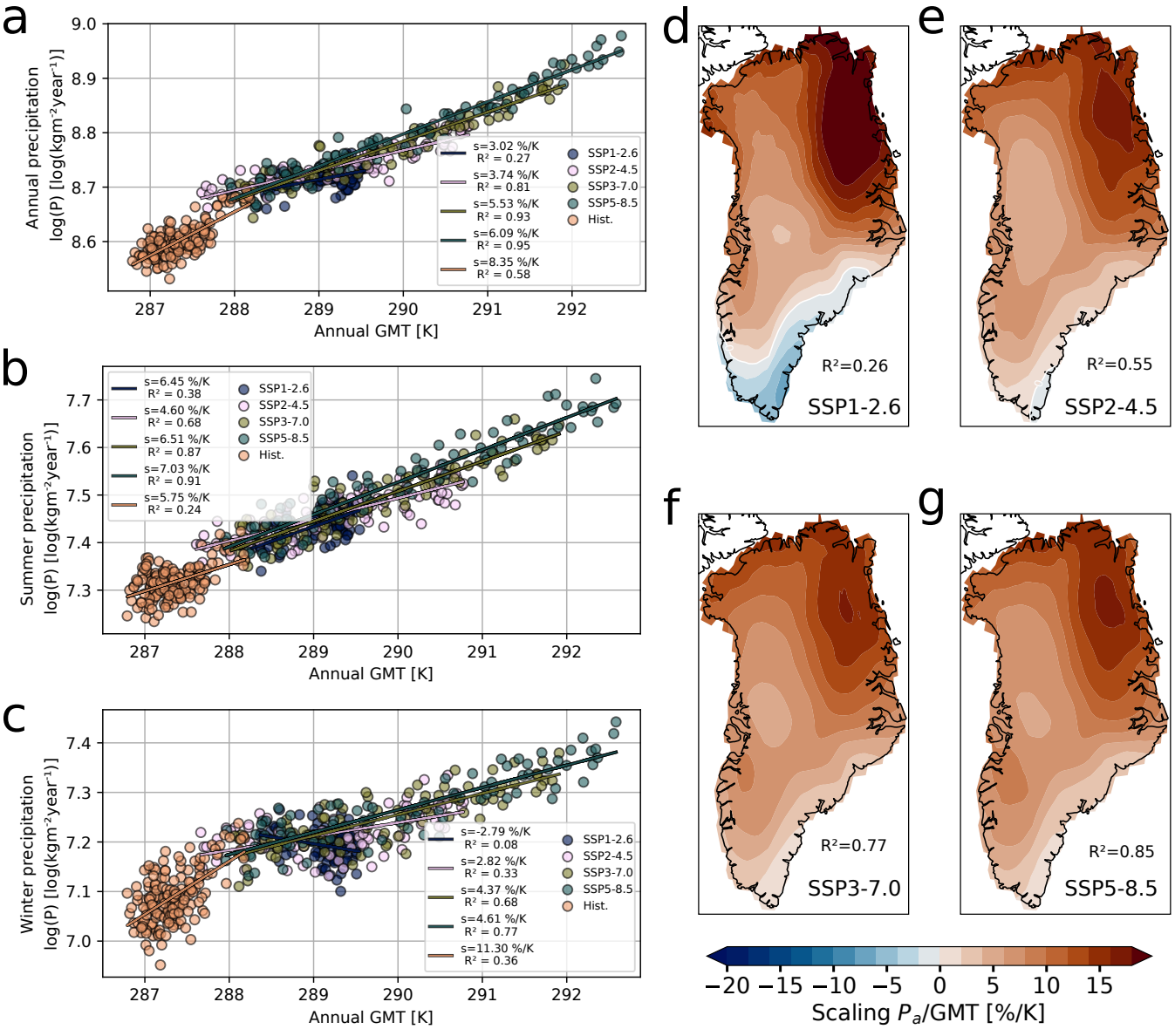

Figure 3. Ensemble mean and spatial scaling factors for precipitation rates relative to global mean temperatures. **(a)** Fit of the ensemble mean of the annual precipitation rates in Greenland against the ensemble mean GMT for all SSP scenarios and the historical time period. **(b,c,)** Same as **a** but for the summer (JJA) and winter (DJF) precipitation rates in Greenland, respectively. The JJA precipitation rates generally increase faster than the DJF precipitation for all scenarios except for the historical time period. **(d)** Regional scaling factors for ensemble mean of annual precipitation rates in Greenland against GMT for SSP1-2.6. The contour at 0%/K denotes the area where the regional precipitation rates decrease. **(e, f, g)** Same as **d** but for SSP2-4.5, SSP3-7.0 and SSP5-8.5, respectively. In all scenarios, precipitation rates increase most strongly in north-eastern Greenland, with a north-south and east-west gradient.

https://doi.org/10.5194/egusphere-2024-1597
Preprint. Discussion started: 27 June 2024

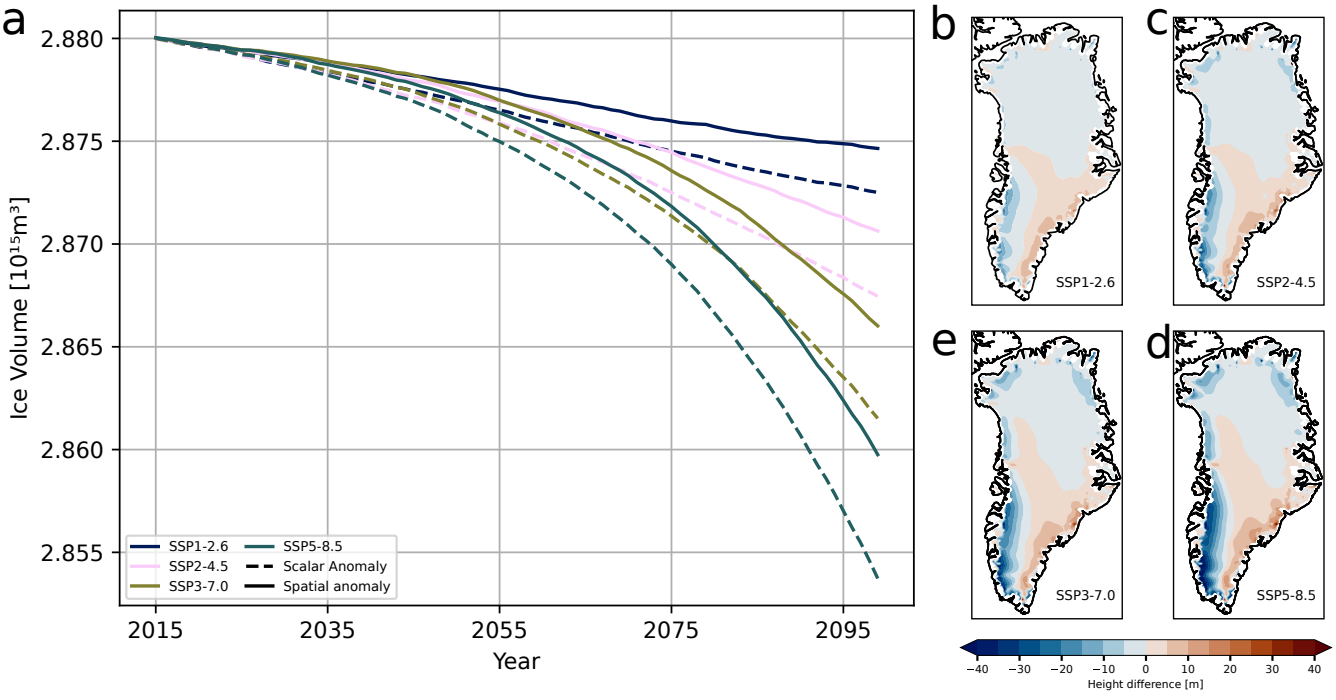

Figure 4. Comparison of simulated short-term ice volume change between scalar and spatially resolved near-surface temperature and precipitation anomalies. **(a)** Simulated ice volume change from 2015 until 2100. PISM is forced with the ensemble mean of the near-surface temperature and precipitation anomalies derived from CMIP6. Solid lines denote the ice volume for spatially resolved anomalies, while the dashed lines denote a spatially uniform scalar anomaly. In each case, the spatially resolved anomalies lead to less ice loss than the scalar anomalies. **(b,c,d,e)** Height difference in the ice thickness in the year 2100 between simulations with spatial and scalar near-surface temperature and precipitation anomalies. Blue areas denote regions where the simulated ice thickness is smaller for the scalar anomalies than for the spatially resolved anomalies. Red areas denote regions where the ice is thicker in the scalar anomaly case. Especially on the southwestern margin of the GrIS, the ice is thinner in the scalar anomaly case in the year 2100. The differences are most pronounced in the SSP5-8.5 scenario.

https://doi.org/10.5194/egusphere-2024-1597
Preprint. Discussion started: 27 June 2024

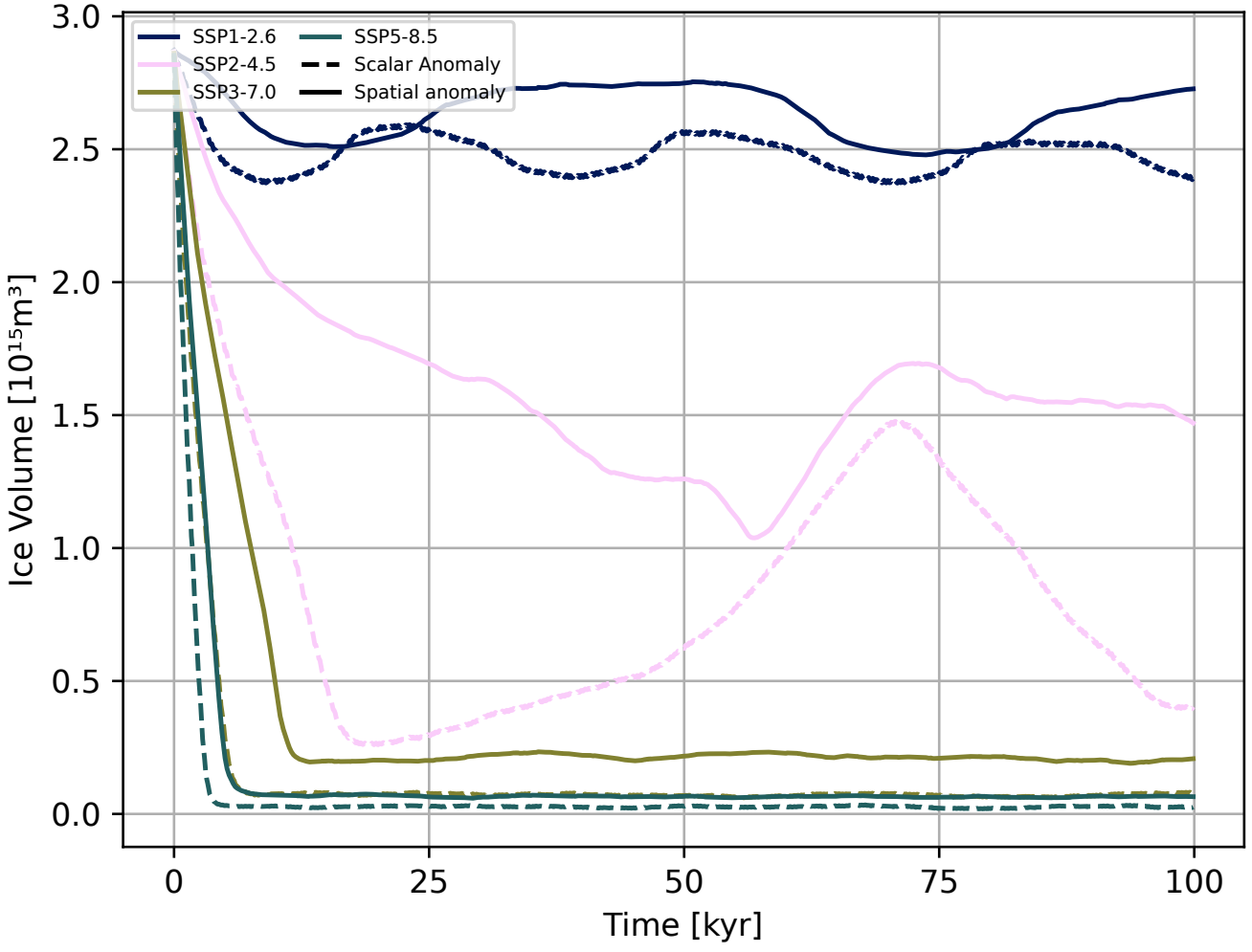

Figure 5. Simulated long-term ice volume for scalar and spatial anomalies. Simulated ice volume with PISM for 100 ka. PISM is forced with the ensemble mean of the near-surface temperature and precipitation anomalies derived from CMIP6 for the years 2090-2100. Solid lines denote the ice volume for spatially resolved anomalies, while the dashed lines denote a uniform anomaly. In each case, the spatially resolved anomalies lead to less ice loss than the scalar anomalies. Oscillations of the ice volume on decamillennial scales is visible.

https://doi.org/10.5194/egusphere-2024-1597
Preprint. Discussion started: 27 June 2024

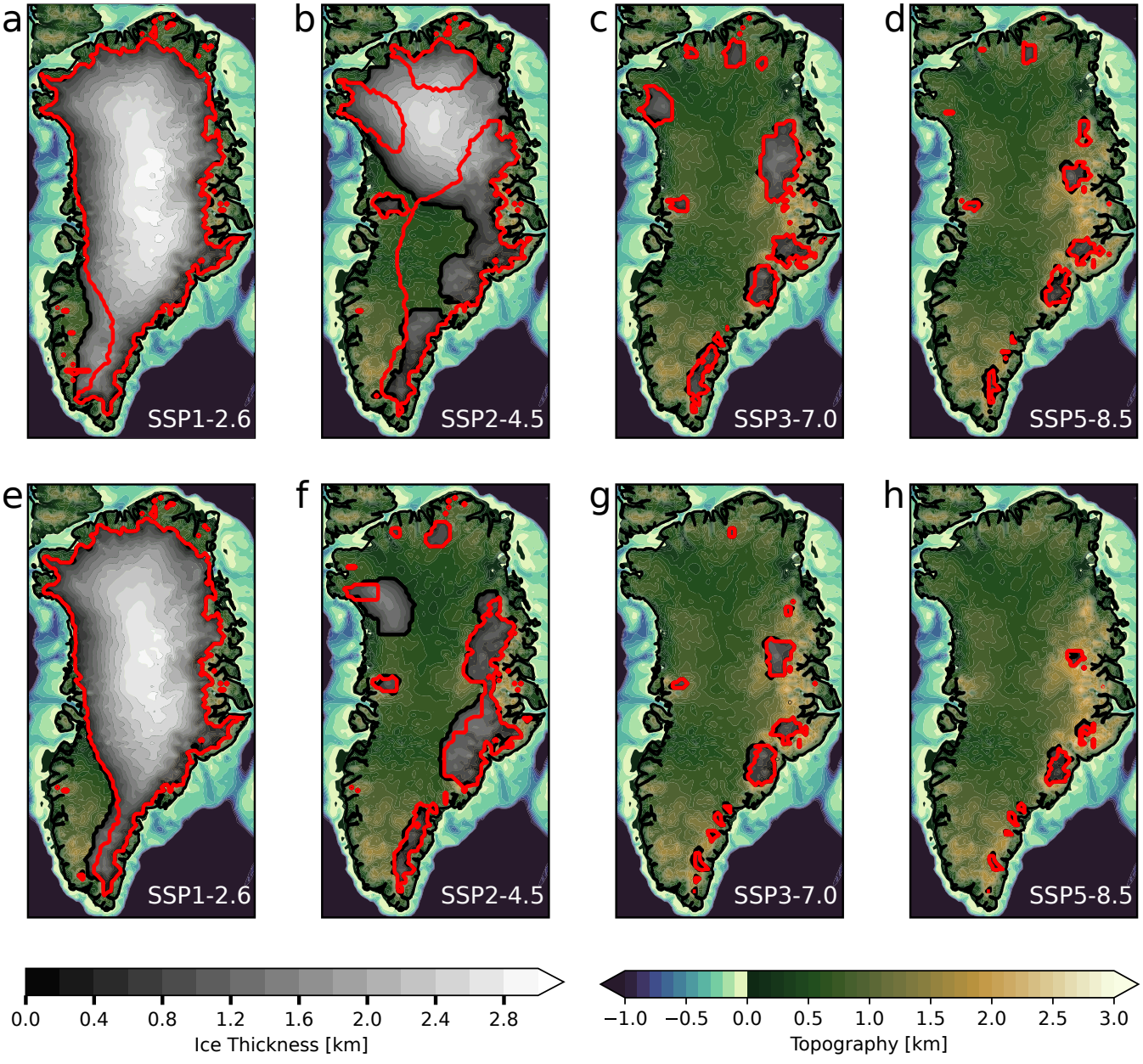

Figure 6. Maps of simulated long-term ice volume for scalar and spatially resolved near-surface temperature and precipitation anomalies. **(a)** Simulated ice volume after 100 ka for the SSP1-2.6 scenario and spatially resolved anomalies. The black outline denotes the ice margin at the end of the simulation while the red line denotes the ice margin of the minimum ice volume within the 100 ka of simulation. **(b, c, d)** Same as **a** but for the SSP2-4.5, SSP3-7.0 and SSP5-8.5 scenario, respectively. **(e, f, g, h)** Same as **a, b, c, d** but for scalar anomalies. The minimum ice volume and the ice volume at the end of the simulation is generally smaller than in the case of spatially resolved anomalies. The differences are very pronounced for the SSP2-4.5 scenario, where a huge mistake would be made when assuming a scalar scaling, while for the more extreme scenarios the ice sheet is completely lost in both cases.

https://doi.org/10.5194/egusphere-2024-1597
Preprint. Discussion started: 27 June 2024

Code and data availability. The CMIP6 data is freely available at https://aims2.llnl.gov/search/cmip6/. The regridded data for Greenland is available on Zenodo at https://doi.org/10.5281/zenodo.11378716. The source code for the ice sheet model PISM is freely available at https://github.com/pism/pism. Scripts used for the analysis are available from the corresponding author upon request.

Appendix A

A1 Temperatures in CMIP6

https://doi.org/10.5194/egusphere-2024-1597
Preprint. Discussion started: 27 June 2024

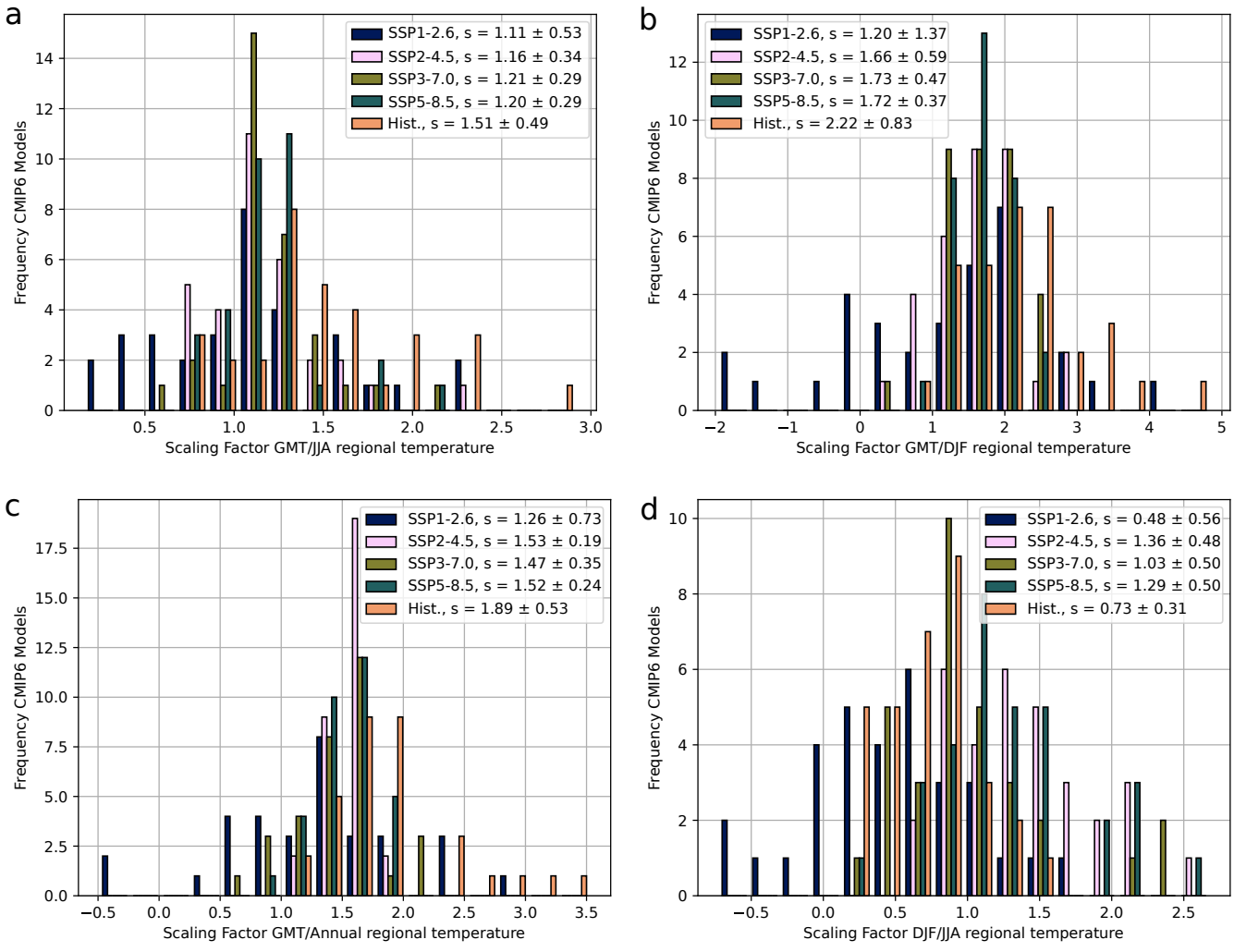

Figure A1. Histograms of seasonal and annual near-surface temperature scaling factors against GMT for all scenarios and models. **(a)** Scaling factors between spatially averaged summer near-surface temperature (JJA) in Greenland and GMT derived from a linear fit for each model and all scenarios. The ensemble mean and standard deviation for each scenario is denoted. **(b)** Same as **a** but for winter temperatures (DJF). The model spread is larger than for summer scaling factors, especially for the SSP1-2.6 scenario. In all cases, the winter near-surface temperature warms faster than the summer temperatures. **(c)** Same as **a** but for mean annual temperatures in Greenland. **(d)** Same as **a** but for scaling factors between regional summer and winter temperatures in Greenland. There is considerable spread in the model response.

https://doi.org/10.5194/egusphere-2024-1597
Preprint. Discussion started: 27 June 2024

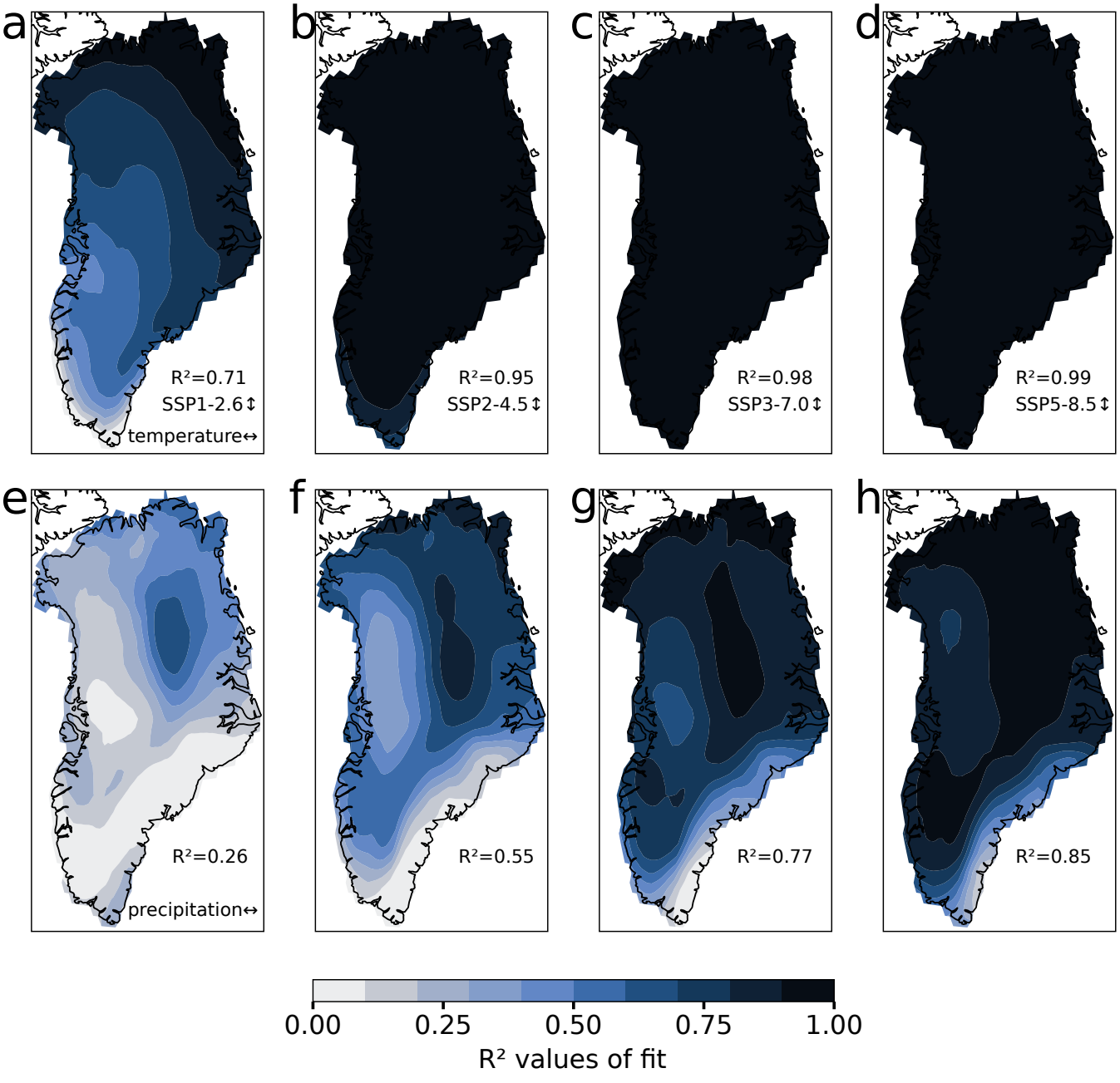

Figure B1. Maps of R^2-values for fit of annual mean temperatures and precipitation rates for all scenarios. (a) Map of R^2-values of linear fit between ensemble mean of regional annual mean near-surface temperature in Greenland and ensemble mean GMT for the SSP1-2.6 scenario. The spatially averaged R^2-value is denoted. There is a clear southwest-northeast gradient with southwest Greenland showing the lowest R^2-values. **(b,c,d)** Same as **a** but for the SSP2-4.5, SSP3-7.0 and SSP5-8.5 scenarios, respectively. **(e,f,g,h)** Same as **a,b,c,d** but for fit of logarithm of ensemble mean precipitation rates against ensemble mean GMT. The ice sheet interior shows the highest R^2-values, while the margins, especially he southeastern margin, show low R^2-values in all scenarios.

https://doi.org/10.5194/egusphere-2024-1597
Preprint. Discussion started: 27 June 2024

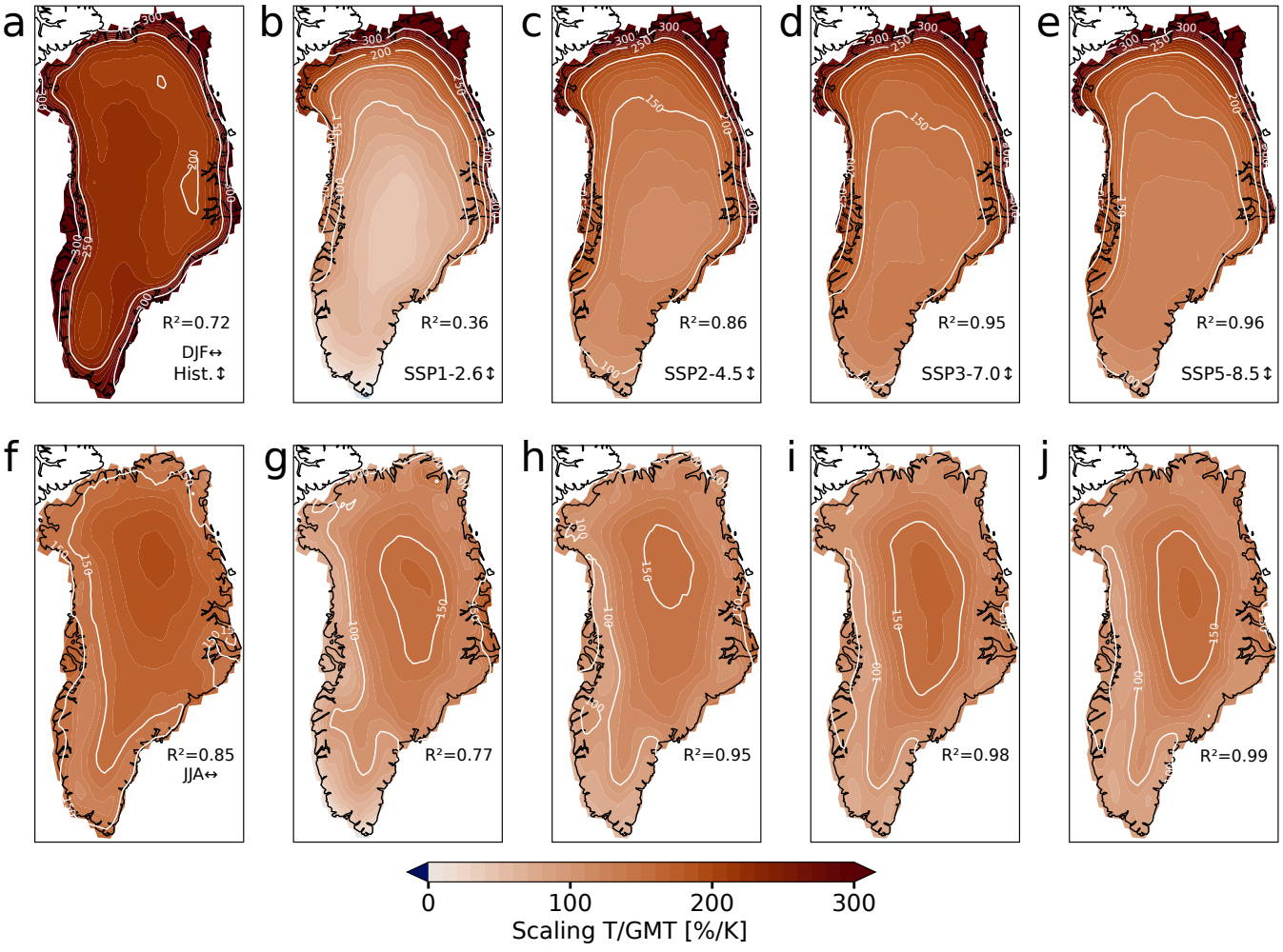

Figure C1. Maps of scaling factors of ensemble mean temperatures in Greenland for winter (DJF) and summer (JJA) and all scenarios. **(a)** Scaling factors between ensemble mean winter temperatures and ensemble mean GMT for the historical period (1850-2015). The margins warm faster than the interior of the ice sheet. The spatially weighted mean R^2-value is denoted. **(b,c,d,e)** Same as **a** but for SSP1-2.6, SSP2-4.5, SSP3-7.0 and SSP5-8.5 scenario, respectively. A clear gradient between southern and northern Greenland is visible, with the northern part warming up to 3 times faster than the southern part. **(f,g,h,i,j)** Same as **a,b,c,d,e** but for ensemble mean summer (JJA) temperatures. In all scenarios, the interior of the ice sheet warms faster than the margins.

https://doi.org/10.5194/egusphere-2024-1597
Preprint. Discussion started: 27 June 2024

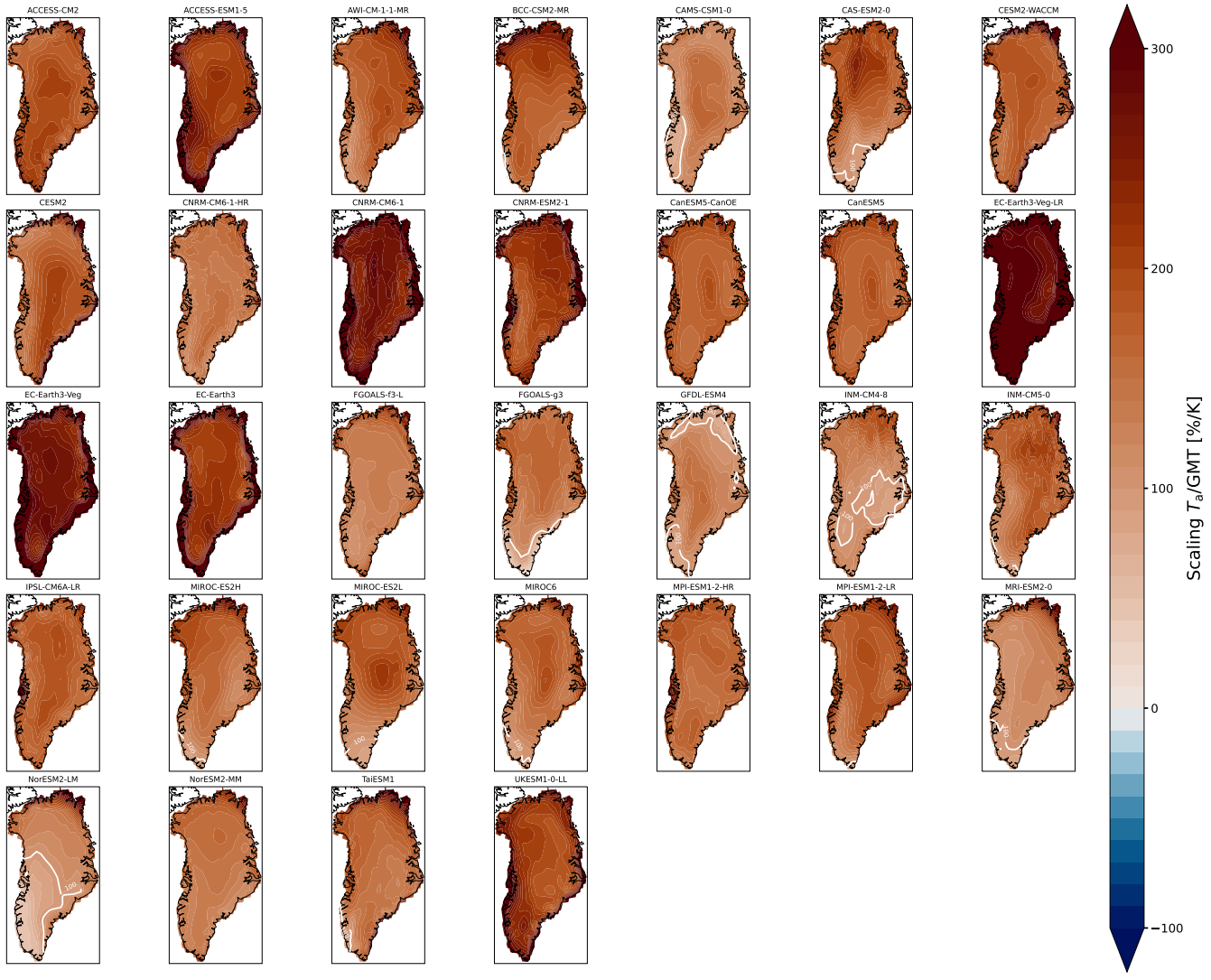

Figure D1. Maps of annual near-surface temperature scaling factors for each CMIP6 model for the historical period. Maps of the annual near-surface temperature scaling factors for all models for the historical period (1850-2015). Most models show a faster warming of Greenland compared to the GMT. The white contour denotes the areas which show a slower increase than the GMT. The spatially weighted R^2-value is denoted for each model.

https://doi.org/10.5194/egusphere-2024-1597
Preprint. Discussion started: 27 June 2024

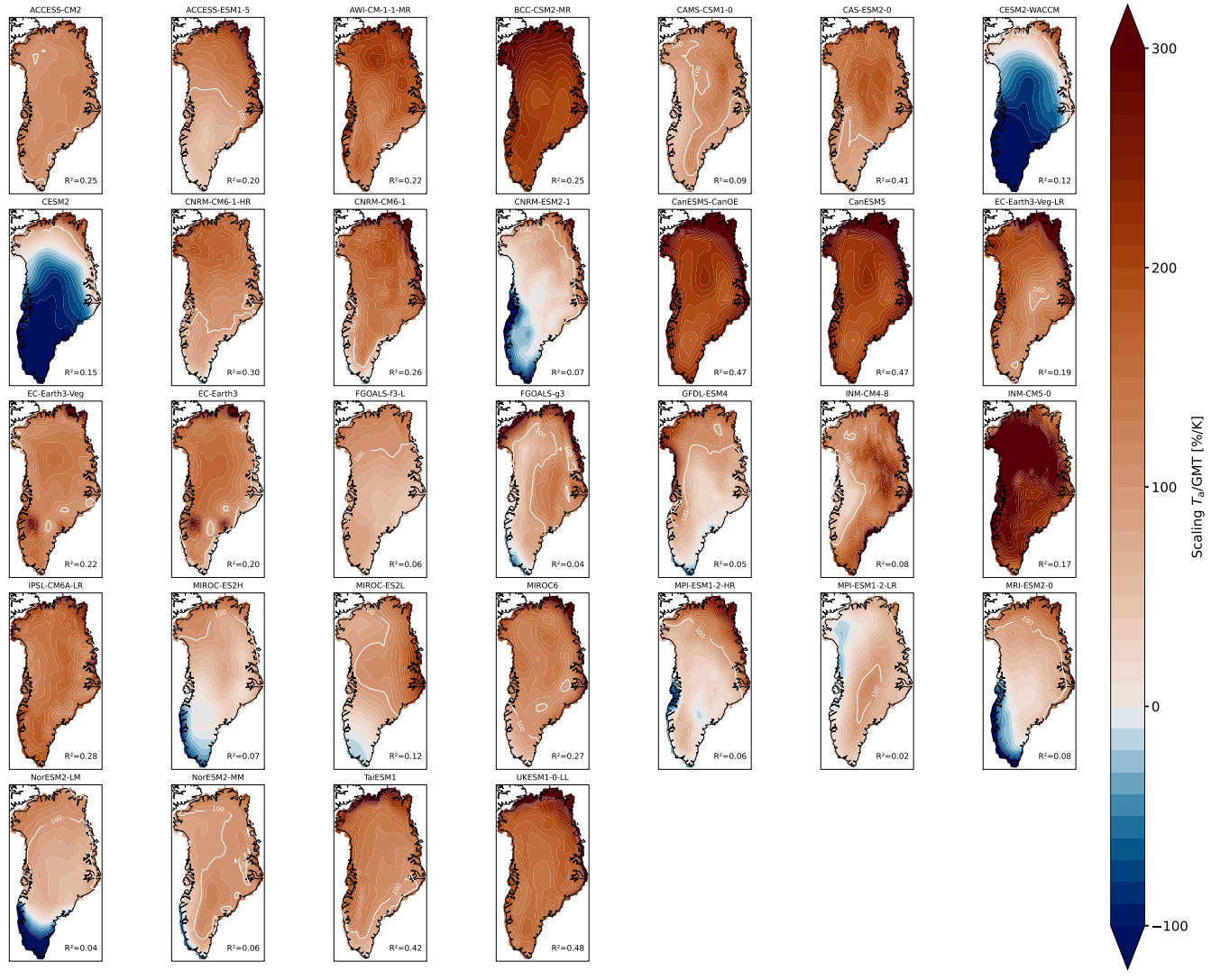

Figure E1. Maps of annual near-surface temperature scaling factors for each CMIP6 model for the SSP1-2.6 scenario. Maps of the annual near-surface temperature scaling factors for all models for the SSP1-2.6 scenario (2015-2100). Most models show a slower warming of most parts of Greenland compared to the GMT. Some models even predict a decrease of the annual temperatures in parts of Greenland. The white contour denotes the areas which show a slower increase than the GMT. The spatially weighted R^2-value is denoted for each model.

https://doi.org/10.5194/egusphere-2024-1597
Preprint. Discussion started: 27 June 2024

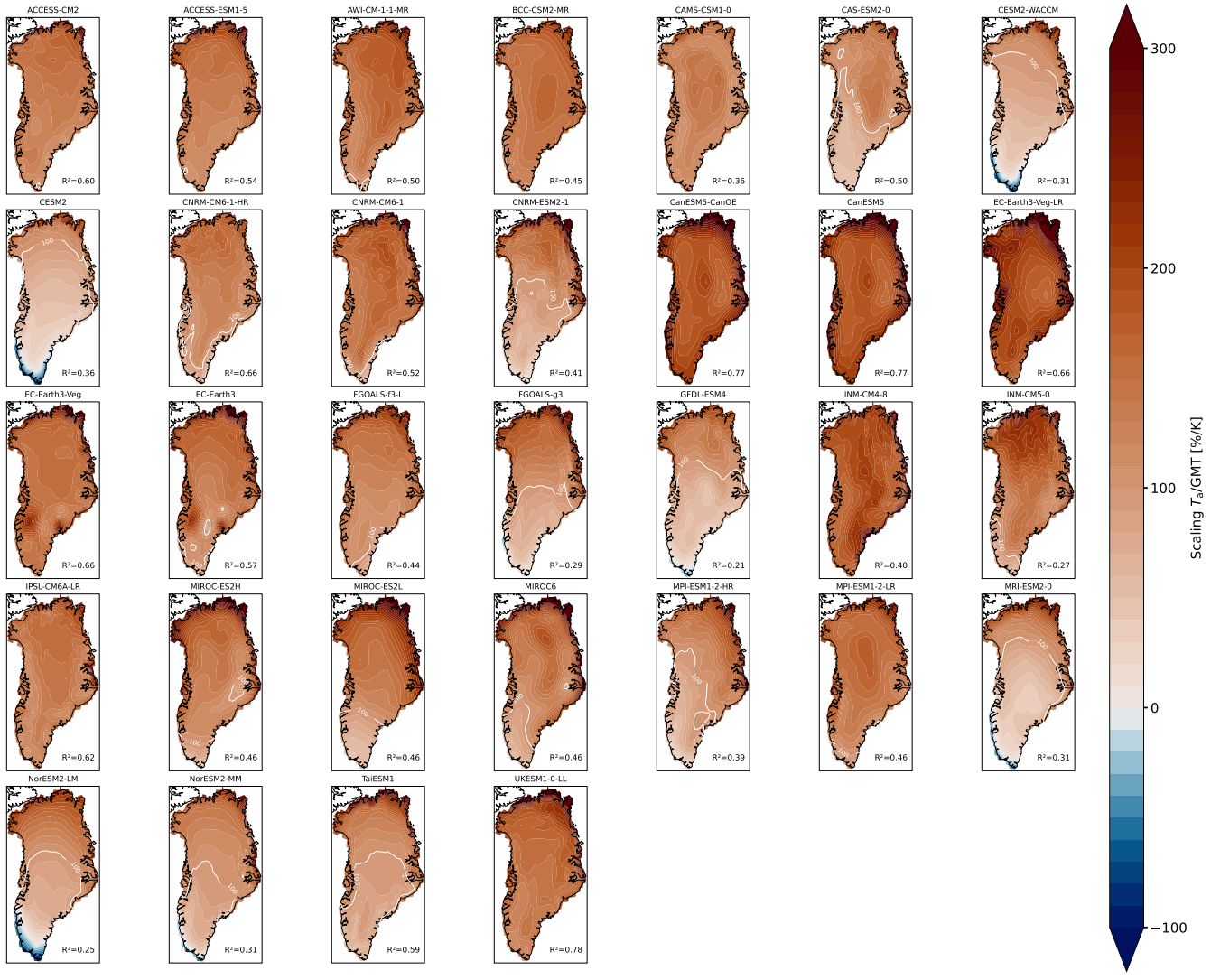

Figure F1. Maps of annual near-surface temperature scaling factors for each CMIP6 model for the SSP2-4.5 scenario. Maps of the annual near-surface temperature scaling factors for all models for the SSP2-4.5 scenario (2015-2100). Most models show a faster warming of most parts of Greenland compared to the GMT. The white contour denotes the areas which show a slower increase than the GMT. The spatially weighted R^2-value is denoted for each model.

https://doi.org/10.5194/egusphere-2024-1597
Preprint. Discussion started: 27 June 2024

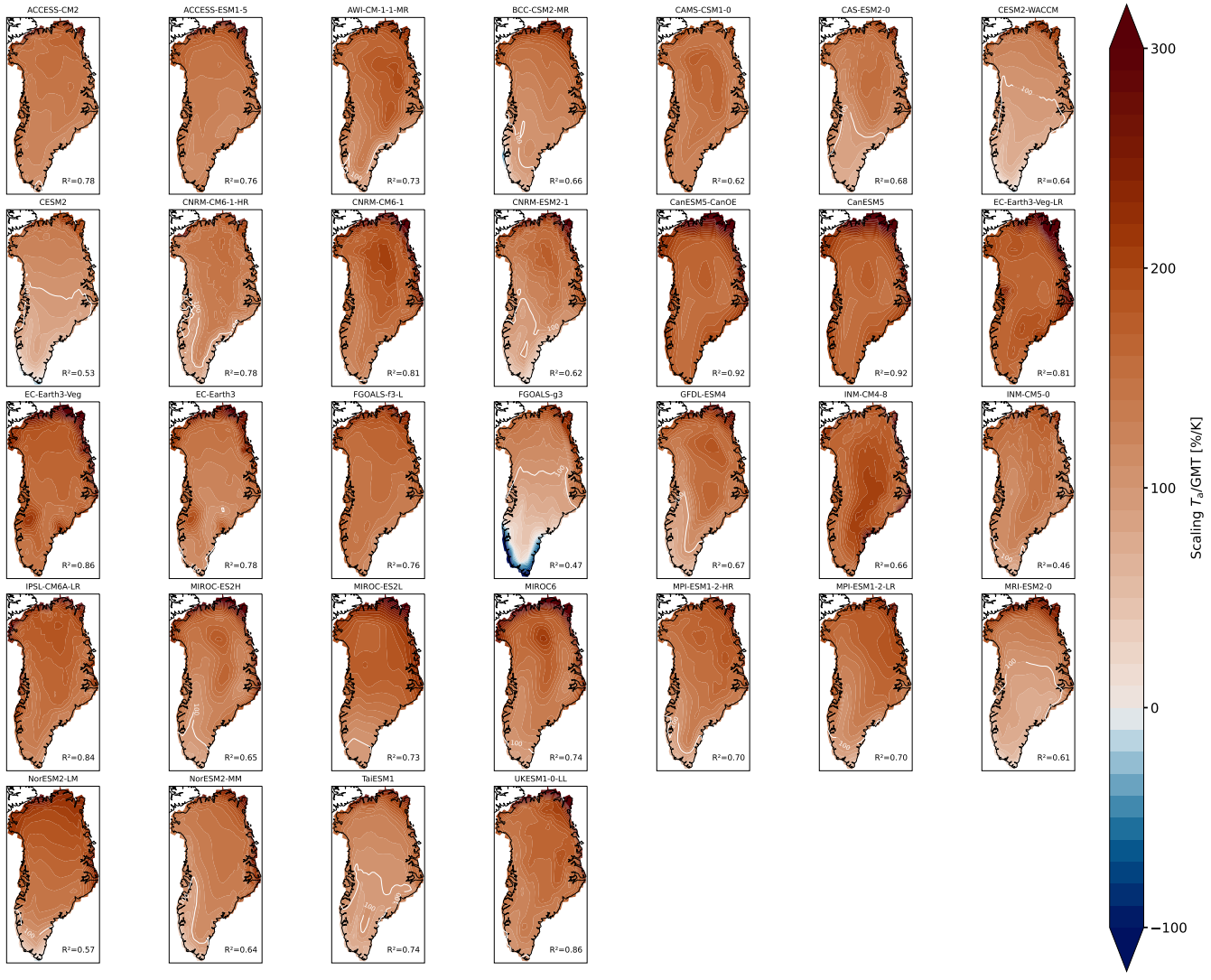

Figure G1. Maps of annual near-surface temperature scaling factors for each CMIP6 model for the SSP3-7.0 scenario. Maps of the annual near-surface temperature scaling factors for all models for the SSP3-7.0 scenario (2015-2100). Most models show a faster warming of most parts of Greenland compared to the GMT. The white contour denotes the areas which show a slower increase than the GMT. The spatially weighted R^2-value is denoted for each model.

https://doi.org/10.5194/egusphere-2024-1597
Preprint. Discussion started: 27 June 2024

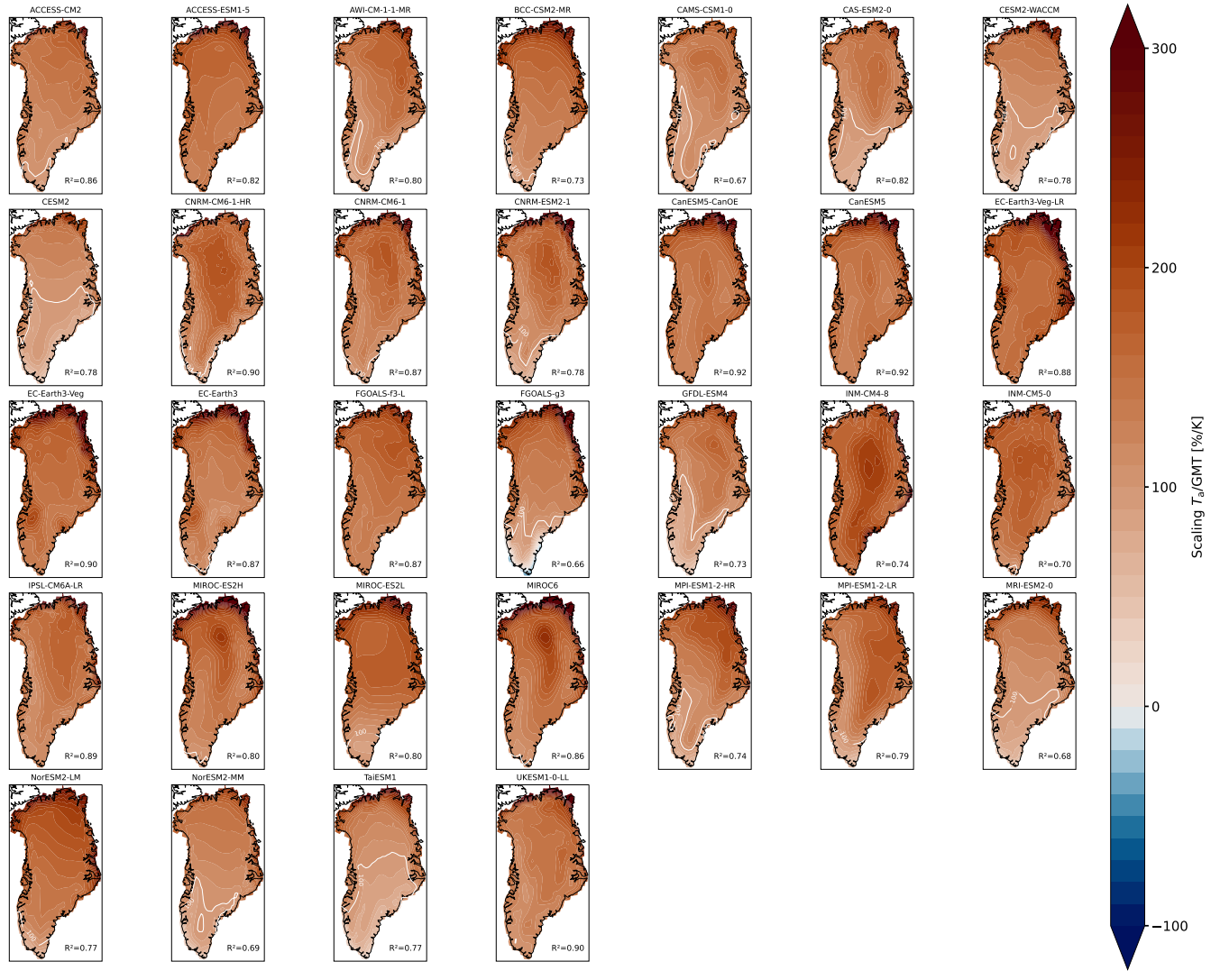

Figure H1. Maps of annual near-surface temperature scaling factors for each CMIP6 model for the SSP5-8.5 scenario. Maps of the annual near-surface temperature scaling factors for all models for the SSP5-8.5 scenario (2015-2100). Most models show a faster warming of whole Greenland compared to the GMT. Some models predict a slower warming of southern Greenland compared to the GMT. The white contour denotes the areas which show a slower increase than the GMT. The spatially weighted R^2-value is denoted for each model.

https://doi.org/10.5194/egusphere-2024-1597
Preprint. Discussion started: 27 June 2024

H1 Precipitation in CMIP6

https://doi.org/10.5194/egusphere-2024-1597
Preprint. Discussion started: 27 June 2024

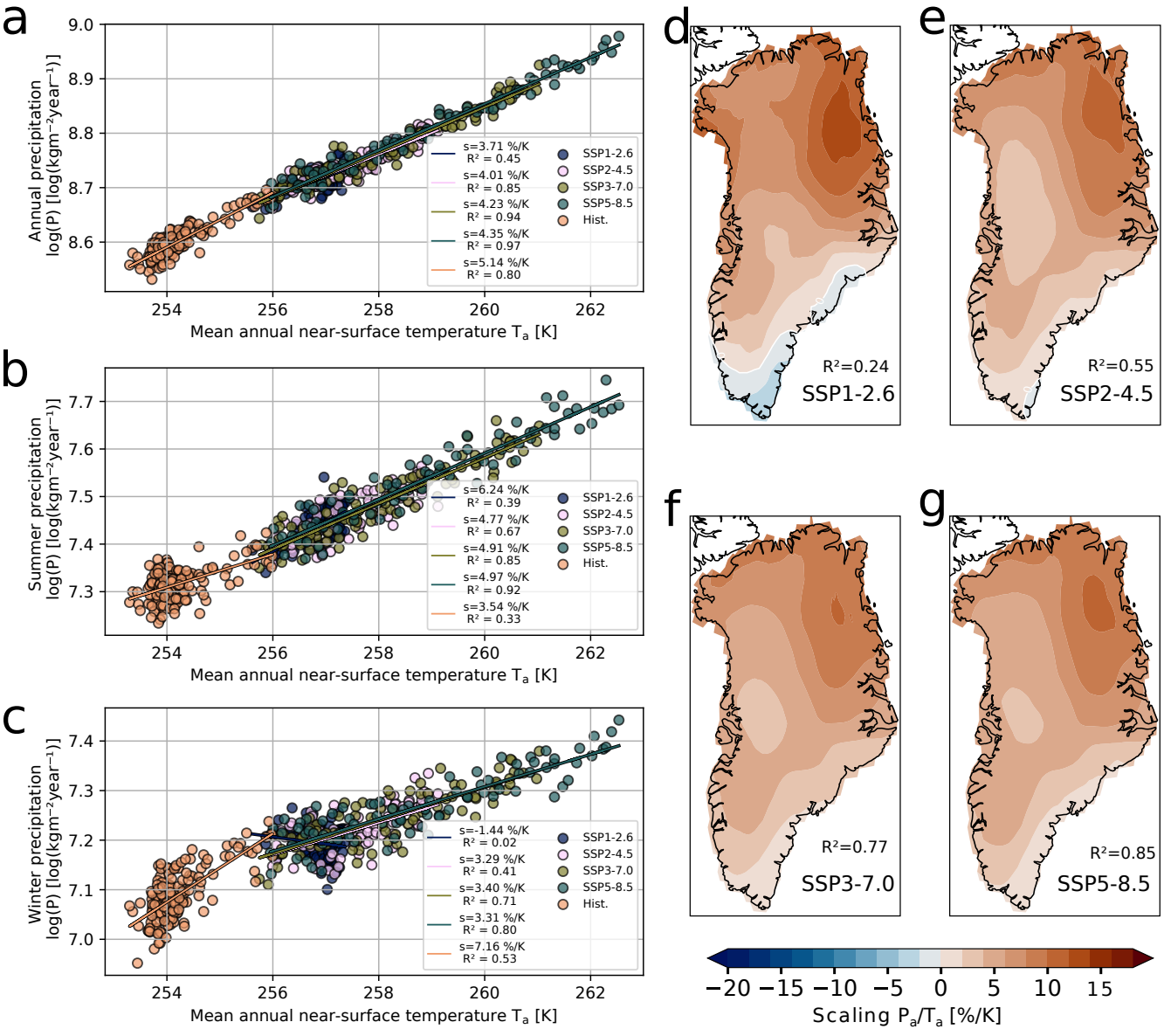

Figure I1. Ensemble mean and spatial scaling factors for precipitation rates relative to annual near-surface temperature in Greenland. **(a)** Fit of the ensemble mean of the annual precipitation rates in Greenland against the ensemble mean annual near-surface temperatures for all SSP scenarios and the historical time period. **(b,c,)** Same as **a** but for the summer (JJA) and winter (DJF) precipitation rates in Greenland, respectively. The JJA precipitation rates generally increase faster than the DJF precipitation for all scenarios except for the historical time period. **(d)** Regional scaling factors for ensemble mean of annual precipitation rates in Greenland against mean annual near-surface temperatures for SSP1-2.6. The contour at 0%/K denotes the area where the regional precipitation rates decrease. **(e, f, g)** Same as **d** but for SSP2-4.5, SSP3-7.0 and SSP5-8.5, respectively. In all scenarios, precipitation rates increase most strongly in north-eastern Greenland, with a north-south and east-west gradient.

https://doi.org/10.5194/egusphere-2024-1597
Preprint. Discussion started: 27 June 2024

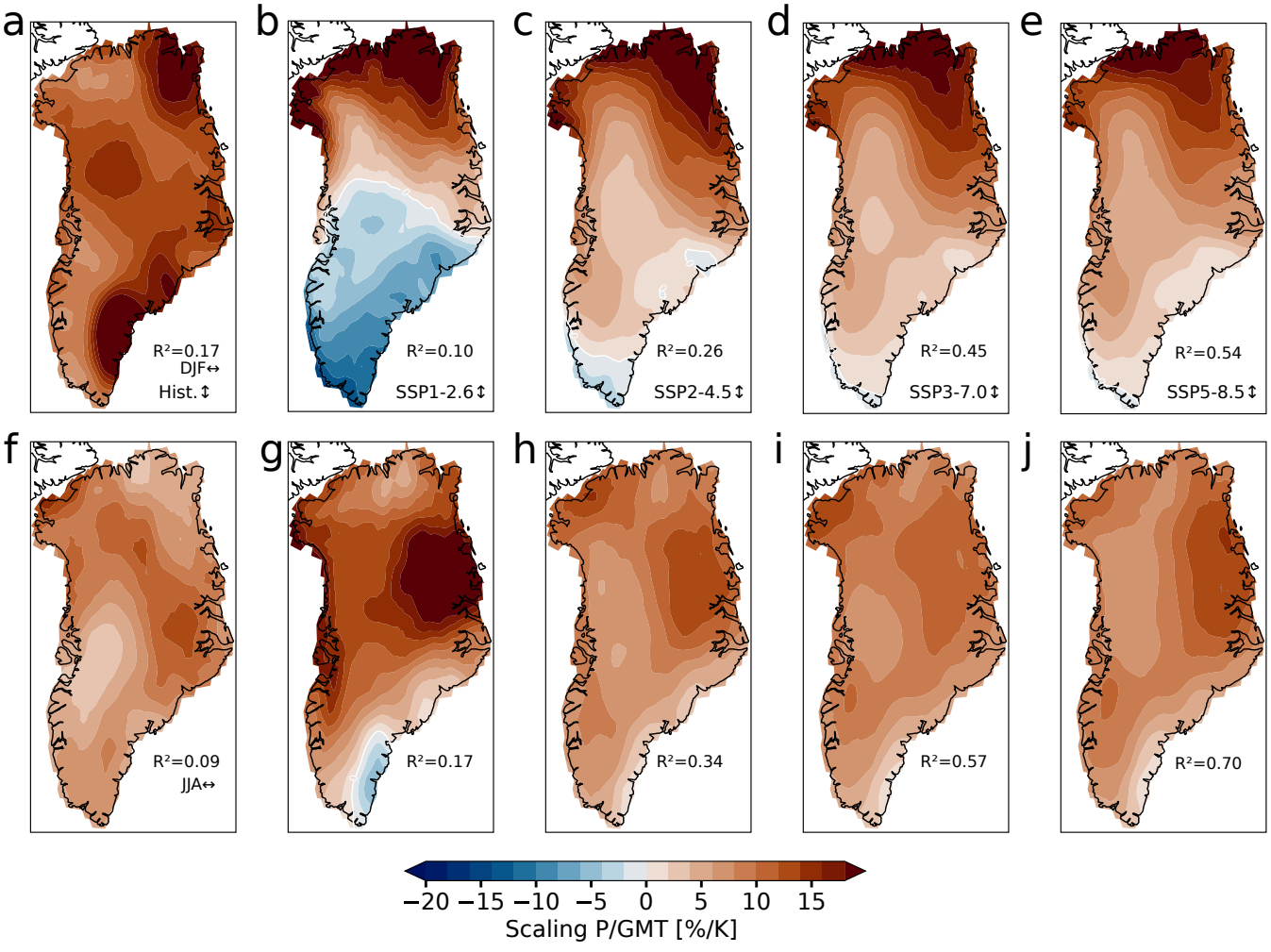

Figure J1. Maps of precipitation sensitivities of ensemble mean precipitation rates for DJF and JJA and all scenarios. **(a)** Precipitation sensitivities of ensemble mean winter precipitation rates and ensemble mean GMT for the historical period (1850-2015). The spatially weighted mean R^2-value is denoted. **(b,c,d,e)** Same as **a** but for SSP1-2.6, SSP2-4.5, SSP3-7.0 and SSP5-8.5 scenario, respectively. A clear gradient between southwestern and northeastern Greenland is visible, with the sensitivities in the northern part exceeding 15%/K. **(f,g,h,i,j)** Same as **a,b,c,d,e** but for ensemble mean summer (JJA) precipitation rates.

https://doi.org/10.5194/egusphere-2024-1597
Preprint. Discussion started: 27 June 2024

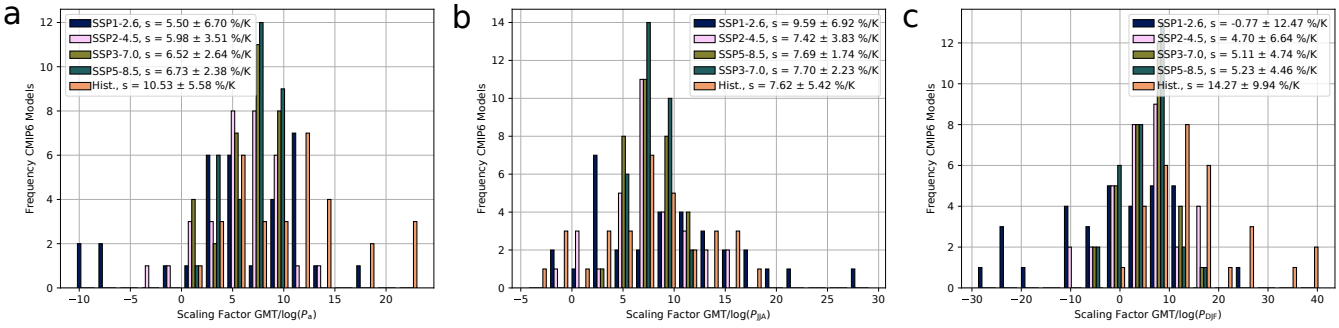

Figure K1. Histograms of seasonal and annual precipitation sensitivities against GMT for all scenarios and models. (a) Sensitivities of spatially averaged annual precipitation rates in Greenland and GMT derived from a linear fit of $\ln(P)$ for each model and all scenarios. The ensemble mean and standard deviation for each scenario is denoted. There is a considerable spread in the model response, especially for the SSP1-2.6 scenario, the uncertainty is larger than the mean. **(b)** Same as **a** but for summer (JJA) precipitation sensitivities. **(c)** Same as **a** but for winter (DJF) precipitation sensitivities in Greenland.

https://doi.org/10.5194/egusphere-2024-1597
Preprint. Discussion started: 27 June 2024

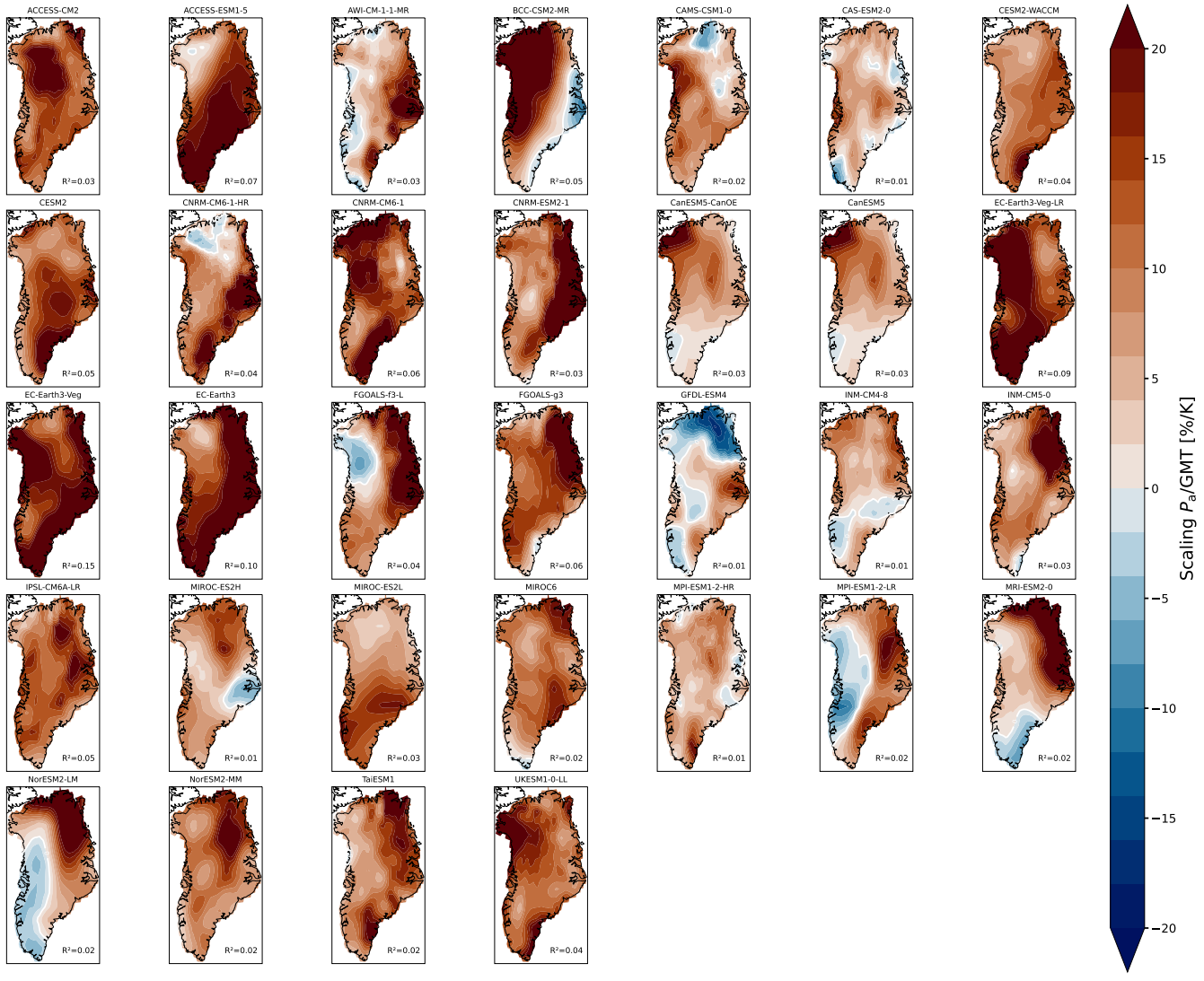

Figure L1. Maps of annual precipitation sensitivities for each CMIP6 model for the historical period. Maps of the precipitation sensitivities for all models for the historical time period (1850-2015). There is no clear pattern in the precipitation sensitivities across the models. The spatially weighted mean R^2-value of the fit is very small for most models. The white contour denotes the areas which show a negative precipitation sensitivity, i.e. a decrease of the precipitation rates. The spatially weighted R^2-value is denoted for each model.

https://doi.org/10.5194/egusphere-2024-1597
Preprint. Discussion started: 27 June 2024

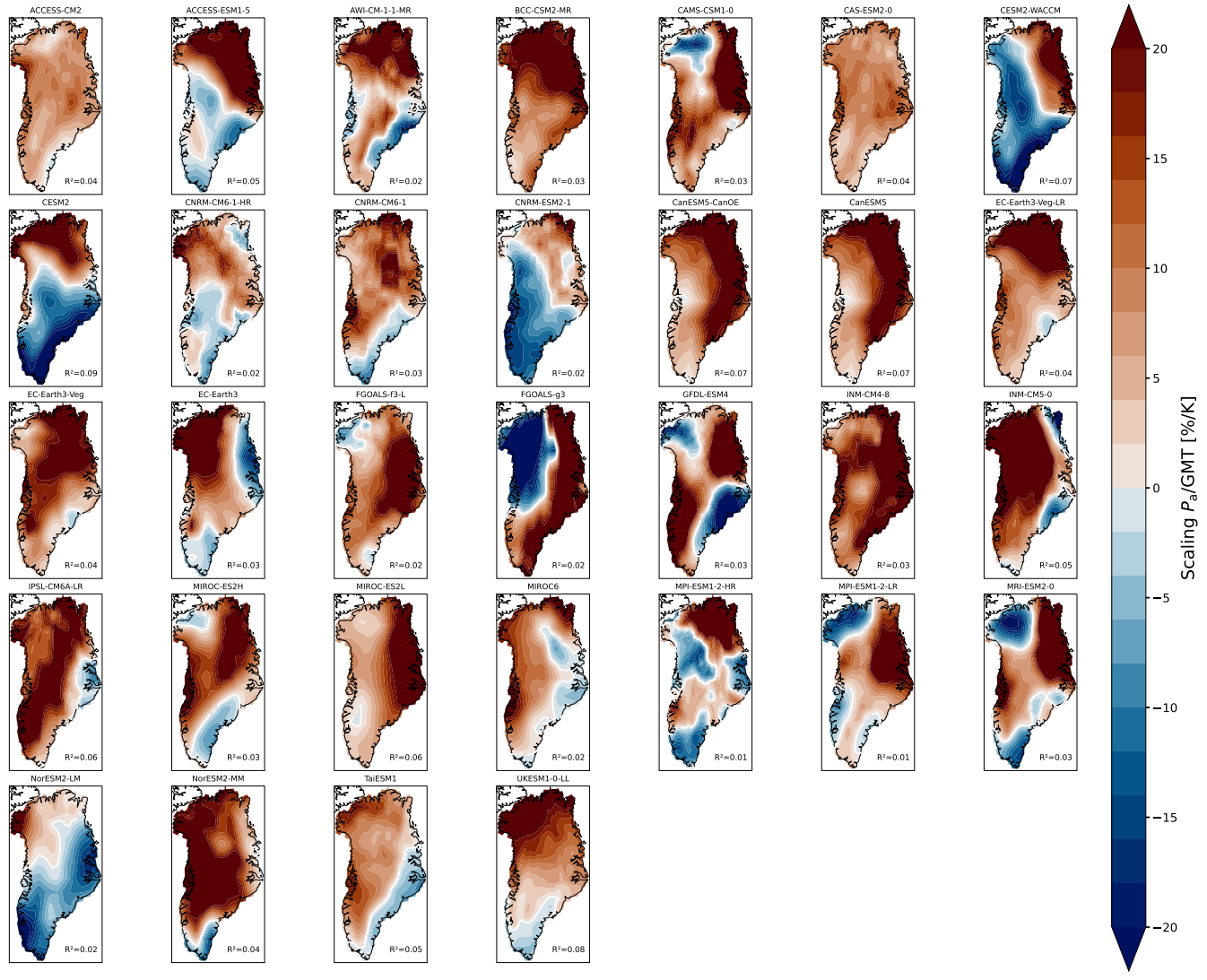

Figure M1. Maps of annual precipitation sensitivities for each CMIP6 model for the SSP1-2.6 scenario. Maps of the precipitation sensitivities for all models for the SSP1-2.6 scenario (2015-2100). There is no clear pattern in the precipitation sensitivities across the models. The spatially weighted mean R^2-value of the fit is very small for most models. The white contour denotes the areas which show a negative precipitation sensitivity, i.e. a decrease of the precipitation rates. The spatially weighted R^2-value is denoted for each model.

https://doi.org/10.5194/egusphere-2024-1597
Preprint. Discussion started: 27 June 2024

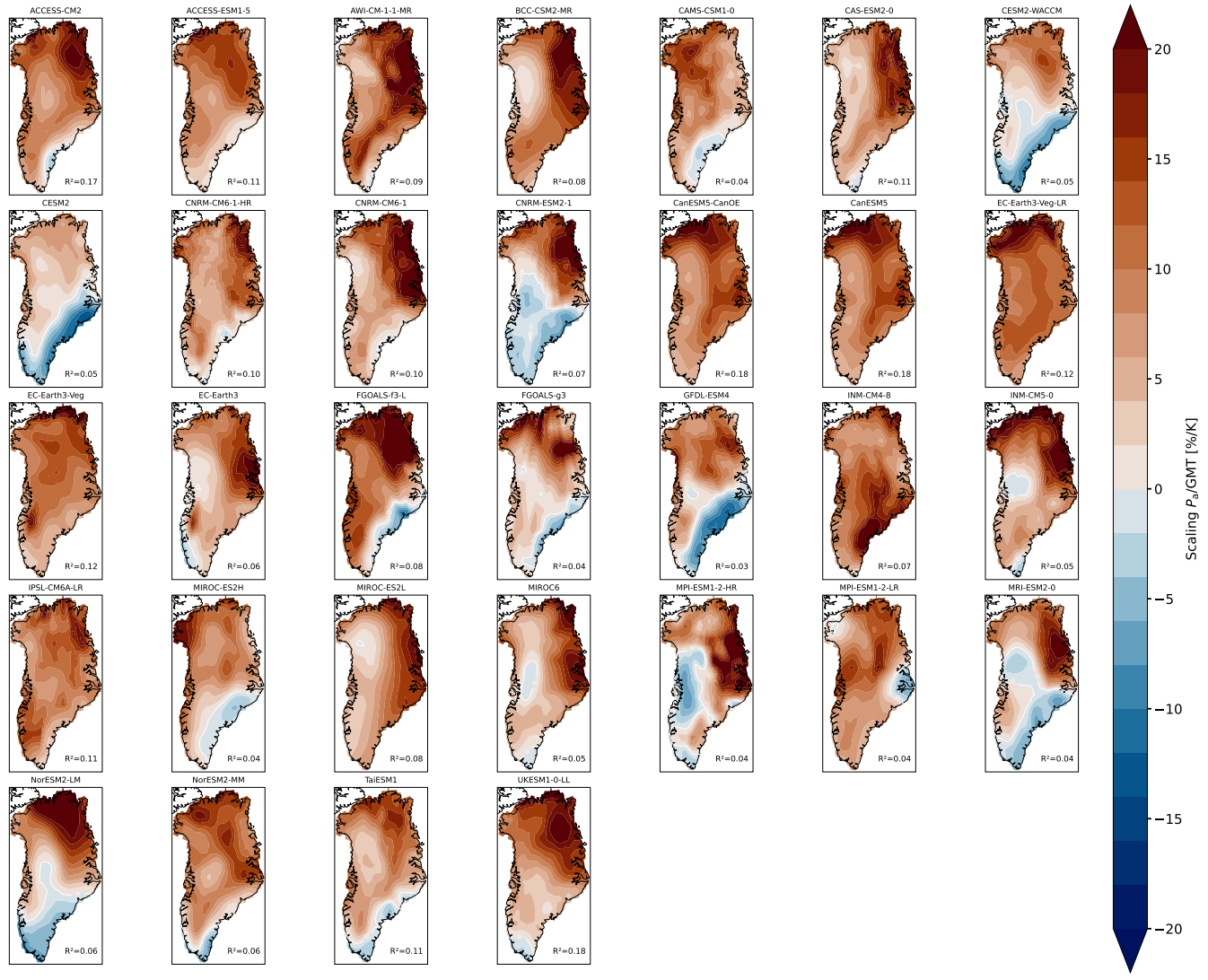

Figure N1. Maps of annual precipitation sensitivities for each CMIP6 model for the SSP2-4.5 scenario. Maps of the precipitation sensitivities for all models for the SSP2-4.5 time period (2015-2100). The majority of models show a positive precipitation sensitivity for most parts of Greenland. However, some models show negative sensitivities for the southeastern margin of the GrIS, partially extending into the interior of the ice sheet. However, the spatially weighted mean R^2-value of the fit is very small for most models. The white contour denotes the areas which show a negative precipitation sensitivity, i.e. a decrease of the precipitation rates. The spatially weighted R^2-value is denoted for each model.

https://doi.org/10.5194/egusphere-2024-1597
Preprint. Discussion started: 27 June 2024

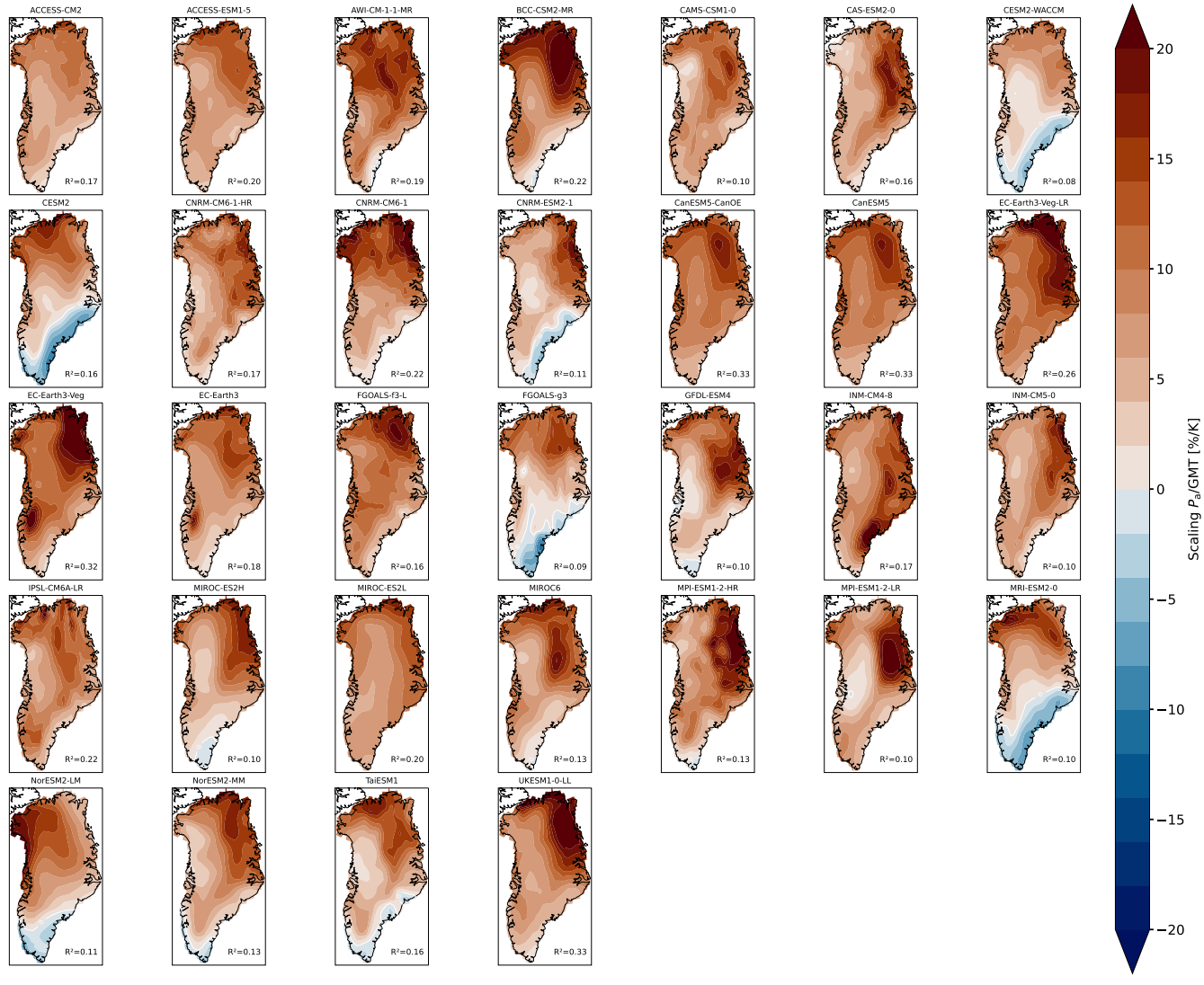

Figure O1. Maps of annual precipitation sensitivities for each CMIP6 model for the SSP3-7.0 scenario. Maps of the precipitation sensitivities for all models for the SSP3-7.0 scenario (2015-2100). The majority of models show a positive precipitation sensitivity for most parts of Greenland. However, some models show negative sensitivities for the southeastern margin of the GrIS. The white contour denotes the areas which show a negative precipitation sensitivity, i.e. a decrease of the precipitation rates. The spatially weighted R^2-value is denoted for each model.

https://doi.org/10.5194/egusphere-2024-1597
Preprint. Discussion started: 27 June 2024

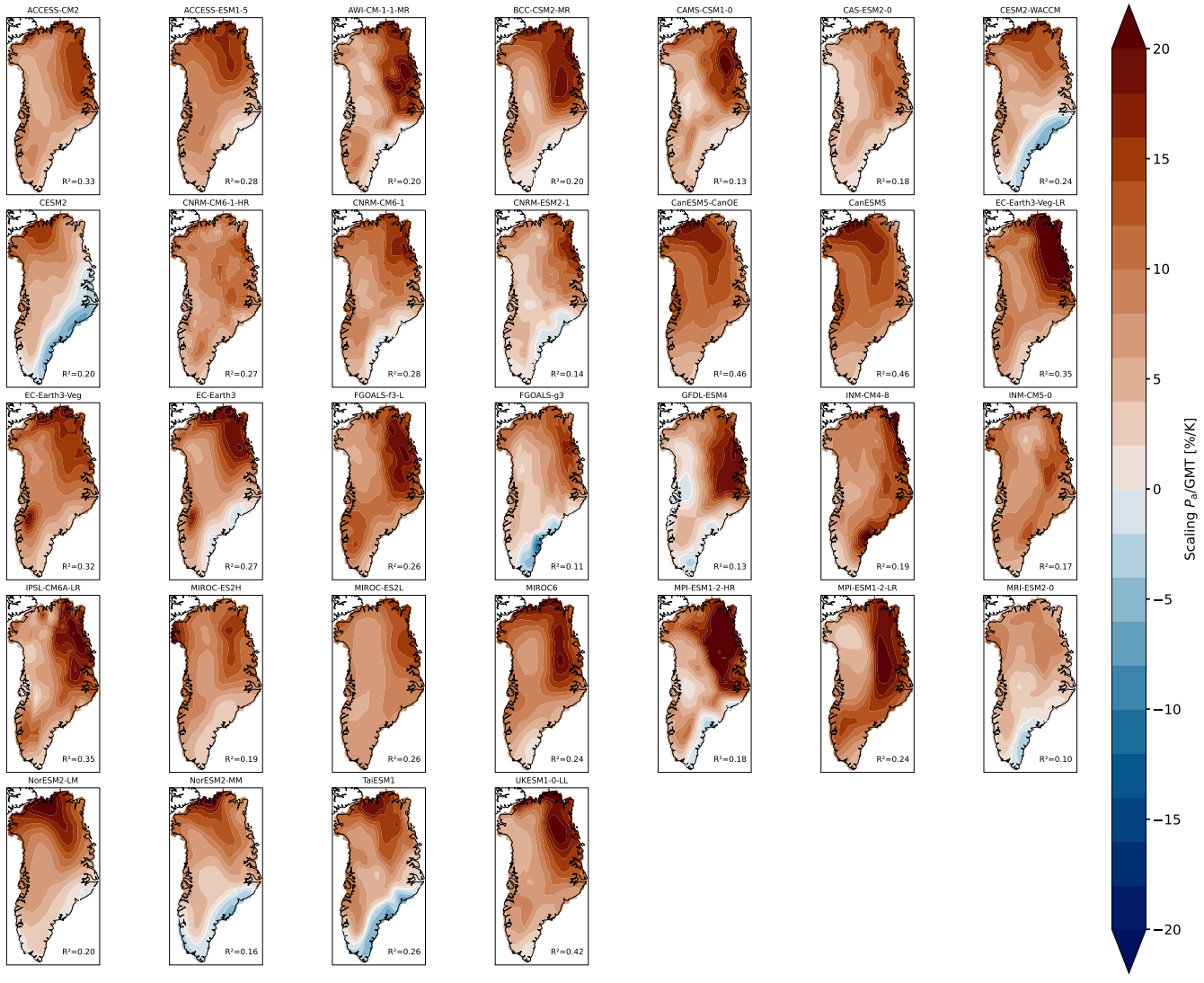

Figure P1. Maps of annual precipitation sensitivities for each CMIP6 model for the SSP5-8.5 scenario. Maps of the precipitation sensitivities for all models for the SSP5-8.5 scenario (2015-2100). The majority of models show a positive precipitation sensitivity for most parts of Greenland. However, some models show negative sensitivities for the southeastern margin of the GrIS. The white contour denotes the areas which show a negative precipitation sensitivity, i.e. a decrease of the precipitation rates. The spatially weighted R^2-value is denoted for each model.

https://doi.org/10.5194/egusphere-2024-1597
Preprint. Discussion started: 27 June 2024

Author contributions. N.Boc. conceived the study. N.Boc. and N.Boe. designed the study. A.P. assembled the CMIP6 data. N.Bow. and A.P. pre-processed the CMIP6 data. N.Boc. did all the analysis and simulations. All authors discussed the results. N.Boc. wrote the manuscript with contributions from all authors.

Competing interests. The authors declare that they have no conflict of interest.

Acknowledgements. This work was supported by the UiT Aurora Centre Program, UiT - The Arctic University of Norway (2020), and the Research Council of Norway (project number 314570). This is ClimTip contribution #8; the ClimTip project has received funding from the European Union's Horizon Europe research and innovation programme under grant agreement No. 101137601. Niklas Boers acknowledges further funding from the Volkswagen Foundation and the European Union's Horizon 2020 research and innovation program under the Marie Sklodowska-Curie grant agreement No. 956170. Parts of the computations were performed on resources provided by Sigma2 - the National Infrastructure for High Performance Computing and Data Storage in Norway under the project nn8008k. The colormaps for the plots are taken from Crameri et al. (2020).

https://doi.org/10.5194/egusphere-2024-1597
Preprint. Discussion started: 27 June 2024

References

Albrecht, T., Winkelmann, R., and Levermann, A.: Glacial-cycle simulations of the Antarctic Ice Sheet with the Parallel Ice Sheet Model (PISM) – Part 2: Parameter ensemble analysis, The Cryosphere, 14, 633–656, https://doi.org/10.5194/tc-14-633-2020, publisher: Copernicus GmbH, 2020.

Armstrong McKay, D. I., Staal, A., Abrams, J. F., Winkelmann, R., Sakschewski, B., Loriani, S., Fetzer, I., Cornell, S. E., Rockström, J., and Lenton, T. M.: Exceeding 1.5°C global warming could trigger multiple climate tipping points, Science, 377, eabn7950, https://doi.org/10.1126/science.abn7950, publisher: American Association for the Advancement of Science, 2022.

Aschwanden, A., Fahnestock, M. A., Truffer, M., Brinkerhoff, D. J., Hock, R., Khroulev, C., Mottram, R., and Khan, S. A.: Contribution of the Greenland Ice Sheet to sea level over the next millennium, Science Advances, 5, eaav9396, https://doi.org/10.1126/sciadv.aav9396, publisher: American Association for the Advancement of Science, 2019.

Auger, J. D., Birkel, S. D., Maasch, K. A., Mayewski, P. A., and Schuenemann, K. C.: Examination of precipitation variability in southern Greenland, Journal of Geophysical Research: Atmospheres, 122, 6202–6216, https://doi.org/10.1002/2016JD026377, _eprint: https://onlinelibrary.wiley.com/doi/pdf/10.1002/2016JD026377, 2017.

Bochow, N., Poltronieri, A., Robinson, A., Montoya, M., Rypdal, M., and Boers, N.: Overshooting the critical threshold for the Greenland ice sheet, Nature, 622, 528–536, https://doi.org/10.1038/s41586-023-06503-9, publisher: Nature Publishing Group, 2023.

Boers, N. and Rypdal, M.: Critical slowing down suggests that the western Greenland Ice Sheet is close to a tipping point, Proceedings of the National Academy of Sciences, 118, https://doi.org/10.1073/pnas.2024192118, publisher: National Academy of Sciences Section: Physical Sciences, 2021.

Bogerd, L., van der Linden, E. C., Krikken, F., and Bintanja, R.: Climate State Dependence of Arctic Precipitation Variability, Journal of Geophysical Research: Atmospheres, 125, e2019JD031 772, https://doi.org/10.1029/2019JD031772, _eprint: https://onlinelibrary.wiley.com/doi/pdf/10.1029/2019JD031772, 2020.

Cappelen, J.: Greenland-DMI historical climate data collection 1784-2019, Tech. rep., Danish Meteorological Institute, 2020.

Choi, Y., Morlighem, M., Rignot, E., and Wood, M.: Ice dynamics will remain a primary driver of Greenland ice sheet mass loss over the next century, Communications Earth & Environment, 2, 1–9, https://doi.org/10.1038/s43247-021-00092-z, publisher: Nature Publishing Group, 2021.

Clausius, R.: Ueber die bewegende Kraft der Wärme und die Gesetze, welche sich daraus für die Wärmelehre selbst ableiten lassen, Annalen der Physik, 155, 368–397, https://doi.org/10.1002/andp.18501550306, _eprint: https://onlinelibrary.wiley.com/doi/pdf/10.1002/andp.18501550306, 1850.

Crameri, F., Shephard, G. E., and Heron, P. J.: The misuse of colour in science communication, Nature Communications, 11, 5444, https://doi.org/10.1038/s41467-020-19160-7, number: 1 Publisher: Nature Publishing Group, 2020.

Crow, B. R., Tarasov, L., Schulz, M., and Prange, M.: Uncertainties originating from GCM downscaling and bias correction with application to the MIS-11c Greenland Ice Sheet, Climate of the Past, 20, 281–296, https://doi.org/10.5194/cp-20-281-2024, publisher: Copernicus GmbH, 2024.

Delhasse, A., Hanna, E., Kittel, C., and Fettweis, X.: Brief communication: CMIP6 does not suggest any atmospheric blocking increase in summer over Greenland by 2100, International Journal of Climatology, 41, 2589–2596, https://doi.org/10.1002/joc.6977, _eprint: https://onlinelibrary.wiley.com/doi/pdf/10.1002/joc.6977, 2021.

https://doi.org/10.5194/egusphere-2024-1597
Preprint. Discussion started: 27 June 2024

Edwards, T. L., Nowicki, S., Marzeion, B., Hock, R., Goelzer, H., Seroussi, H., Jourdain, N. C., Slater, D. A., Turner, F. E., Smith, C. J., McKenna, C. M., Simon, E., Abe-Ouchi, A., Gregory, J. M., Larour, E., Lipscomb, W. H., Payne, A. J., Shepherd, A., Agosta, C., Alexander, P., Albrecht, T., Anderson, B., Asay-Davis, X., Aschwanden, A., Barthel, A., Bliss, A., Calov, R., Chambers, C., Champollion, N., Choi, Y., Cullather, R., Cuzzone, J., Dumas, C., Felikson, D., Fettweis, X., Fujita, K., Galton-Fenzi, B. K., Gladstone, R., Golledge, N. R., Greve, R., Hattermann, T., Hoffman, M. J., Humbert, A., Huss, M., Huybrechts, P., Immerzeel, W., Kleiner, T., Kraaijenbrink, P., Le clec'h, S., Lee, V., Leguy, G. R., Little, C. M., Lowry, D. P., Malles, J.-H., Martin, D. F., Maussion, F., Morlighem, M., O'Neill, J. F., Nias, I., Pattyn, F., Pelle, T., Price, S. F., Quiquet, A., Radić, V., Reese, R., Rounce, D. R., Rückamp, M., Sakai, A., Shafer, C., Schlegel, N.-J., Shannon, S., Smith, R. S., Straneo, F., Sun, S., Tarasov, L., Trusel, L. D., Van Breedam, J., van de Wal, R., van den Broeke, M., Winkelmann, R., Zekollari, H., Zhao, C., Zhang, T., and Zwinger, T.: Projected land ice contributions to twenty-first-century sea level rise, Nature, 593, 74–82, https://doi.org/10.1038/s41586-021-03302-y, publisher: Nature Publishing Group, 2021.

Erokhina, O., Rogozhina, I., Prange, M., Bakker, P., Bernales, J., Paul, A., and Schulz, M.: Dependence of slope lapse rate over the Greenland ice sheet on background climate, Journal of Glaciology, 63, 568–572, https://doi.org/10.1017/jog.2017.10, 2017.

Fettweis, X., Box, J. E., Agosta, C., Amory, C., Kittel, C., Lang, C., van As, D., Machguth, H., and Gallée, H.: Reconstructions of the 1900–2015 Greenland ice sheet surface mass balance using the regional climate MAR model, The Cryosphere, 11, 1015–1033, https://doi.org/10.5194/tc-11-1015-2017, publisher: Copernicus GmbH, 2017.

Frieler, K., Meinshausen, M., Mengel, M., Braun, N., and Hare, W.: A Scaling Approach to Probabilistic Assessment of Regional Climate Change, Journal of Climate, 25, 3117–3144, https://doi.org/10.1175/JCLI-D-11-00199.1, publisher: American Meteorological Society Section: Journal of Climate, 2012.

Frieler, K., Clark, P. U., He, F., Buizert, C., Reese, R., Ligtenberg, S. R. M., van den Broeke, M. R., Winkelmann, R., and Levermann, A.: Consistent evidence of increasing Antarctic accumulation with warming, Nature Climate Change, 5, 348–352, https://doi.org/10.1038/nclimate2574, publisher: Nature Publishing Group, 2015.

Garbe, J., Albrecht, T., Levermann, A., Donges, J. F., and Winkelmann, R.: The hysteresis of the Antarctic Ice Sheet, Nature, 585, 538–544, https://doi.org/10.1038/s41586-020-2727-5, number: 7826 Publisher: Nature Publishing Group, 2020.

Garbe, J., Zeitz, M., Krebs-Kanzow, U., and Winkelmann, R.: The evolution of future Antarctic surface melt using PISM-dEBM-simple, The Cryosphere, 17, 4571–4599, https://doi.org/10.5194/tc-17-4571-2023, publisher: Copernicus GmbH, 2023.

Goelzer, H., Nowicki, S., Payne, A., Larour, E., Seroussi, H., Lipscomb, W. H., Gregory, J., Abe-Ouchi, A., Shepherd, A., Simon, E., Agosta, C., Alexander, P., Aschwanden, A., Barthel, A., Calov, R., Chambers, C., Choi, Y., Cuzzone, J., Dumas, C., Edwards, T., Felikson, D., Fettweis, X., Golledge, N. R., Greve, R., Humbert, A., Huybrechts, P., Le clec'h, S., Lee, V., Leguy, G., Little, C., Lowry, D. P., Morlighem, M., Nias, I., Quiquet, A., Rückamp, M., Schlegel, N.-J., Slater, D. A., Smith, R. S., Straneo, F., Tarasov, L., van de Wal, R., and van den Broeke, M.: The future sea-level contribution of the Greenland ice sheet: a multi-model ensemble study of ISMIP6, The Cryosphere, 14, 3071–3096, https://doi.org/10.5194/tc-14-3071-2020, publisher: Copernicus GmbH, 2020.

Gregory, J. M., George, S. E., and Smith, R. S.: Large and irreversible future decline of the Greenland ice sheet, The Cryosphere, 14, 4299–4322, https://doi.org/10.5194/tc-14-4299-2020, publisher: Copernicus GmbH, 2020.

Groves, D. G. and Francis, J. A.: Variability of the Arctic atmospheric moisture budget from TOVS satellite data, Journal of Geophysical Research: Atmospheres, 107, ACL 18–1–ACL 18–15, https://doi.org/10.1029/2002JD002285, _eprint: https://onlinelibrary.wiley.com/doi/pdf/10.1029/2002JD002285, 2002.

Held, I. M. and Soden, B. J.: Robust Responses of the Hydrological Cycle to Global Warming, Journal of Climate, 19, 5686–5699, https://doi.org/10.1175/JCLI3990.1, publisher: American Meteorological Society Section: Journal of Climate, 2006.

https://doi.org/10.5194/egusphere-2024-1597
Preprint. Discussion started: 27 June 2024

Henderson-Sellers, B.: A new formula for latent heat of vaporization of water as a function of temperature, Quarterly Journal of the Royal Meteorological Society, 110, 1186–1190, https://doi.org/10.1002/qj.49711046626, _eprint: https://onlinelibrary.wiley.com/doi/pdf/10.1002/qj.49711046626, 1984.

Huybrechts, P.: Sea-level changes at the LGM from ice-dynamic reconstructions of the Greenland and Antarctic ice sheets during the glacial cycles, Quaternary Science Reviews, 21, 203–231, https://epic.awi.de/id/eprint/4507/, number: 1, 2002.

Höning, D., Willeit, M., Calov, R., Klemann, V., Bagge, M., and Ganopolski, A.: Multistability and Transient Response of the Greenland Ice Sheet to Anthropogenic CO2 Emissions, Geophysical Research Letters, 50, e2022GL101 827, https://doi.org/10.1029/2022GL101827, _eprint: https://onlinelibrary.wiley.com/doi/pdf/10.1029/2022GL101827, 2023.

Höning, D., Willeit, M., and Ganopolski, A.: Reversibility of Greenland ice sheet mass loss under artificial carbon dioxide removal scenarios, Environmental Research Letters, 19, 024 038, https://doi.org/10.1088/1748-9326/ad2129, publisher: IOP Publishing, 2024.

Jiang, S., Ye, A., and Xiao, C.: The temperature increase in Greenland has accelerated in the past five years, Global and Planetary Change, 194, 103 297, https://doi.org/10.1016/j.gloplacha.2020.103297, 2020.

Jordahl, K., Bossche, J. V. d., Fleischmann, M., Wasserman, J., McBride, J., Gerard, J., Tratner, J., Perry, M., Badaracco, A. G., Farmer, C., Hjelle, G. A., Snow, A. D., Cochran, M., Gillies, S., Culbertson, L., Bartos, M., Eubank, N., maxalbert, Bilogur, A., Rey, S., Ren, C., Arribas-Bel, D., Wasser, L., Wolf, L. J., Journois, M., Wilson, J., Greenhall, A., Holdgraf, C., Filipe, and Leblanc, F.: geopandas/geopandas: v0.8.1, https://doi.org/10.5281/zenodo.3946761, 2020.

Krebs-Kanzow, U., Gierz, P., and Lohmann, G.: Brief communication: An ice surface melt scheme including the diurnal cycle of solar radiation, The Cryosphere, 12, 3923–3930, https://doi.org/10.5194/tc-12-3923-2018, publisher: Copernicus GmbH, 2018.

Krebs-Kanzow, U., Gierz, P., Rodehacke, C. B., Xu, S., Yang, H., and Lohmann, G.: The diurnal Energy Balance Model (dEBM): a convenient surface mass balance solution for ice sheets in Earth system modeling, The Cryosphere, 15, 2295–2313, https://doi.org/10.5194/tc-15-2295-2021, publisher: Copernicus GmbH, 2021.

Levermann, A. and Winkelmann, R.: A simple equation for the melt elevation feedback of ice sheets, The Cryosphere, 10, 1799–1807, https://doi.org/10.5194/tc-10-1799-2016, publisher: Copernicus GmbH, 2016.

Lewis, G., Osterberg, E., Hawley, R., Whitmore, B., Marshall, H. P., and Box, J.: Regional Greenland accumulation variability from Operation IceBridge airborne accumulation radar, The Cryosphere, 11, 773–788, https://doi.org/10.5194/tc-11-773-2017, publisher: Copernicus GmbH, 2017.

Lewis, G., Osterberg, E., Hawley, R., Marshall, H. P., Meehan, T., Graeter, K., McCarthy, F., Overly, T., Thundercloud, Z., and Ferris, D.: Recent precipitation decrease across the western Greenland ice sheet percolation zone, The Cryosphere, 13, 2797–2815, https://doi.org/10.5194/tc-13-2797-2019, publisher: Copernicus GmbH, 2019.

Lliboutry, L. and Duval, P.: Various isotropic and anisotropic ices found in glaciers and polar ice caps and their corresponding rheologies: Ann Geophys V3, N2, March–April 1985, P207–224, International Journal of Rock Mechanics and Mining Sciences & Geomechanics Abstracts, 22, 198, https://doi.org/10.1016/0148-9062(85)90267-0, 1985.

Madsen, M. S., Yang, S., Aðalgeirsdóttir, G., Svendsen, S. H., Rodehacke, C. B., and Ringgaard, I. M.: The role of an interactive Greenland ice sheet in the coupled climate-ice sheet model EC-Earth-PISM, Climate Dynamics, 59, 1189–1211, https://doi.org/10.1007/s00382-022-06184-6, 2022.

Mernild, S. H., Hanna, E., McConnell, J. R., Sigl, M., Beckerman, A. P., Yde, J. C., Cappelen, J., Malmros, J. K., and Steffen, K.: Greenland precipitation trends in a long-term instrumental climate context (1890–2012): evaluation of coastal and ice core records, International

https://doi.org/10.5194/egusphere-2024-1597
Preprint. Discussion started: 27 June 2024

Journal of Climatology, 35, 303–320, https://doi.org/10.1002/joc.3986, _eprint: https://onlinelibrary.wiley.com/doi/pdf/10.1002/joc.3986, 2015.

Morlighem, M., Williams, C. N., Rignot, E., An, L., Arndt, J. E., Bamber, J. L., Catania, G., Chauché, N., Dowdeswell, J. A., Dorschel, B., Fenty, I., Hogan, K., Howat, I., Hubbard, A., Jakobsson, M., Jordan, T. M., Kjeldsen, K. K., Millan, R., Mayer, L., Mouginot, J., Noël, B. P. Y., O'Cofaigh, C., Palmer, S., Rysgaard, S., Seroussi, H., Siegert, M. J., Slabon, P., Straneo, F., van den Broeke, M. R., Weinrebe, W., Wood, M., and Zinglersen, K. B.: BedMachine v3: Complete Bed Topography and Ocean Bathymetry Mapping of Greenland From Multibeam Echo Sounding Combined With Mass Conservation, Geophysical Research Letters, 44, 11,051–11,061, https://doi.org/10.1002/2017GL074954, _eprint: https://onlinelibrary.wiley.com/doi/pdf/10.1002/2017GL074954, 2017.

Muntjewerf, L., Petrini, M., Vizcaino, M., Ernani da Silva, C., Sellevold, R., Scherrenberg, M. D. W., Thayer-Calder, K., Bradley, S. L., Lenaerts, J. T. M., Lipscomb, W. H., and Lofverstrom, M.: Greenland Ice Sheet Contribution to 21st Century Sea Level Rise as Simulated by the Coupled CESM2.1-CISM2.1, Geophysical Research Letters, 47, e2019GL086 836, https://doi.org/10.1029/2019GL086836, _eprint: https://onlinelibrary.wiley.com/doi/pdf/10.1029/2019GL086836, 2020a.

Muntjewerf, L., Sellevold, R., Vizcaino, M., Ernani da Silva, C., Petrini, M., Thayer-Calder, K., Scherrenberg, M. D. W., Bradley, S. L., Katsman, C. A., Fyke, J., Lipscomb, W. H., Lofverstrom, M., and Sacks, W. J.: Accelerated Greenland Ice Sheet Mass Loss Under High Greenhouse Gas Forcing as Simulated by the Coupled CESM2.1-CISM2.1, Journal of Advances in Modeling Earth Systems, 12, e2019MS002 031, https://doi.org/10.1029/2019MS002031, _eprint: https://onlinelibrary.wiley.com/doi/pdf/10.1029/2019MS002031, 2020b.

Nicola, L., Notz, D., and Winkelmann, R.: Revisiting temperature sensitivity: how does Antarctic precipitation change with temperature?, The Cryosphere, 17, 2563–2583, https://doi.org/10.5194/tc-17-2563-2023, publisher: Copernicus GmbH, 2023.

Otosaka, I. N., Shepherd, A., Ivins, E. R., Schlegel, N.-J., Amory, C., van den Broeke, M. R., Horwath, M., Joughin, I., King, M. D., Krinner, G., Nowicki, S., Payne, A. J., Rignot, E., Scambos, T., Simon, K. M., Smith, B. E., Sørensen, L. S., Velicogna, I., Whitehouse, P. L., A, G., Agosta, C., Ahlstrøm, A. P., Blazquez, A., Colgan, W., Engdahl, M. E., Fettweis, X., Forsberg, R., Gallée, H., Gardner, A., Gilbert, L., Gourmelen, N., Groh, A., Gunter, B. C., Harig, C., Helm, V., Khan, S. A., Kittel, C., Konrad, H., Langen, P. L., Lecavalier, B. S., Liang, C.-C., Loomis, B. D., McMillan, M., Melini, D., Mernild, S. H., Mottram, R., Mouginot, J., Nilsson, J., Noël, B., Pattle, M. E., Peltier, W. R., Pie, N., Roca, M., Sasgen, I., Save, H. V., Seo, K.-W., Scheuchl, B., Schrama, E. J. O., Schröder, L., Simonsen, S. B., Slater, T., Spada, G., Sutterley, T. C., Vishwakarma, B. D., van Wessem, J. M., Wiese, D., van der Wal, W., and Wouters, B.: Mass balance of the Greenland and Antarctic ice sheets from 1992 to 2020, Earth System Science Data, 15, 1597–1616, https://doi.org/10.5194/essd-15-1597-2023, publisher: Copernicus GmbH, 2023.

Payne, A. J., Nowicki, S., Abe-Ouchi, A., Agosta, C., Alexander, P., Albrecht, T., Asay-Davis, X., Aschwanden, A., Barthel, A., Bracegirdle, T. J., Calov, R., Chambers, C., Choi, Y., Cullather, R., Cuzzone, J., Dumas, C., Edwards, T. L., Felikson, D., Fettweis, X., Galton-Fenzi, B. K., Goelzer, H., Gladstone, R., Golledge, N. R., Gregory, J. M., Greve, R., Hattermann, T., Hoffman, M. J., Humbert, A., Huybrechts, P., Jourdain, N. C., Kleiner, T., Munneke, P. K., Larour, E., Le clec'h, S., Lee, V., Leguy, G., Lipscomb, W. H., Little, C. M., Lowry, D. P., Morlighem, M., Nias, I., Pattyn, F., Pelle, T., Price, S. F., Quiquet, A., Reese, R., Rückamp, M., Schlegel, N.-J., Seroussi, H., Shepherd, A., Simon, E., Slater, D., Smith, R. S., Straneo, F., Sun, S., Tarasov, L., Trusel, L. D., Van Breedam, J., van de Wal, R., van den Broeke, M., Winkelmann, R., Zhao, C., Zhang, T., and Zwinger, T.: Future Sea Level Change Under Coupled Model Intercomparison Project Phase 5 and Phase 6 Scenarios From the Greenland and Antarctic Ice Sheets, Geophysical Research Letters, 48, e2020GL091 741, https://doi.org/10.1029/2020GL091741, _eprint: https://onlinelibrary.wiley.com/doi/pdf/10.1029/2020GL091741, 2021.

https://doi.org/10.5194/egusphere-2024-1597
Preprint. Discussion started: 27 June 2024

Petrini, M., Scherrenberg, M., Muntjewerf, L., Vizcaino, M., Sellevold, R., Leguy, G., Lipscomb, W., and Goelzer, H.: A topographically-controlled tipping point for complete Greenland ice-sheet melt, The Cryosphere Discussions, pp. 1–28, https://doi.org/10.5194/tc-2023-154, publisher: Copernicus GmbH, 2023.

Preece, J. R., Mote, T. L., Cohen, J., Wachowicz, L. J., Knox, J. A., Tedesco, M., and Kooperman, G. J.: Summer atmospheric circulation over Greenland in response to Arctic amplification and diminished spring snow cover, Nature Communications, 14, 3759, https://doi.org/10.1038/s41467-023-39466-6, publisher: Nature Publishing Group, 2023.

Rantanen, M., Karpechko, A. Y., Lipponen, A., Nordling, K., Hyvärinen, O., Ruosteenoja, K., Vihma, T., and Laaksonen, A.: The Arctic has warmed nearly four times faster than the globe since 1979, Communications Earth & Environment, 3, 1–10, https://doi.org/10.1038/s43247-022-00498-3, publisher: Nature Publishing Group, 2022.

Riahi, K., van Vuuren, D. P., Kriegler, E., Edmonds, J., O'Neill, B. C., Fujimori, S., Bauer, N., Calvin, K., Dellink, R., Fricko, O., Lutz, W., Popp, A., Cuaresma, J. C., Kc, S., Leimbach, M., Jiang, L., Kram, T., Rao, S., Emmerling, J., Ebi, K., Hasegawa, T., Havlik, P., Humpenöder, F., Da Silva, L. A., Smith, S., Stehfest, E., Bosetti, V., Eom, J., Gernaat, D., Masui, T., Rogelj, J., Strefler, J., Drouet, L., Krey, V., Luderer, G., Harmsen, M., Takahashi, K., Baumstark, L., Doelman, J. C., Kainuma, M., Klimont, Z., Marangoni, G., Lotze-Campen, H., Obersteiner, M., Tabeau, A., and Tavoni, M.: The Shared Socioeconomic Pathways and their energy, land use, and greenhouse gas emissions implications: An overview, Global Environmental Change, 42, 153–168, https://doi.org/10.1016/j.gloenvcha.2016.05.009, 2017.

Robinson, A., Calov, R., and Ganopolski, A.: Multistability and critical thresholds of the Greenland ice sheet, Nature Climate Change, 2, 429–432, https://doi.org/10.1038/nclimate1449, number: 6 Publisher: Nature Publishing Group, 2012.

Rodehacke, C. B., Pfeiffer, M., Semmler, T., Gurses, \., and Kleiner, T.: Future sea level contribution from Antarctica inferred from CMIP5 model forcing and its dependence on precipitation ansatz, Earth System Dynamics, 11, 1153–1194, https://doi.org/10.5194/esd-11-1153-2020, publisher: Copernicus GmbH, 2020.

Saito, F., Abe-Ouchi, A., Takahashi, K., and Blatter, H.: SeaRISE experiments revisited: potential sources of spread in multi-model projections of the Greenland ice sheet, The Cryosphere, 10, 43–63, https://doi.org/10.5194/tc-10-43-2016, publisher: Copernicus GmbH, 2016.

Schoof, C. and Hindmarsh, R. C. A.: Thin-Film Flows with Wall Slip: An Asymptotic Analysis of Higher Order Glacier Flow Models, The Quarterly Journal of Mechanics and Applied Mathematics, 63, 73–114, https://doi.org/10.1093/qjmam/hbp025, 2010.

Schulzweida, U.: CDO user guide, https://doi.org/10.5281/zenodo.10020800, tex.version: 2.3.0, 2023.

Screen, J. A. and Simmonds, I.: The central role of diminishing sea ice in recent Arctic temperature amplification, Nature, 464, 1334–1337, https://doi.org/10.1038/nature09051, publisher: Nature Publishing Group, 2010.

Serreze, M. C. and Barry, R. G.: Processes and impacts of Arctic amplification: A research synthesis, Global and Planetary Change, 77, 85–96, https://doi.org/10.1016/j.gloplacha.2011.03.004, 2011.

Shapiro, N. M. and Ritzwoller, M. H.: Inferring surface heat flux distributions guided by a global seismic model: particular application to Antarctica, Earth and Planetary Science Letters, 223, 213–224, https://doi.org/10.1016/j.epsl.2004.04.011, 2004.

Shepherd, A., Ivins, E., Rignot, E., Smith, B., van den Broeke, M., Velicogna, I., Whitehouse, P., Briggs, K., Joughin, I., Krinner, G., Nowicki, S., Payne, T., Scambos, T., Schlegel, N., A, G., Agosta, C., Ahlstrøm, A., Babonis, G., Barletta, V. R., Bjørk, A. A., Blazquez, A., Bonin, J., Colgan, W., Csatho, B., Cullather, R., Engdahl, M. E., Felikson, D., Fettweis, X., Forsberg, R., Hogg, A. E., Gallee, H., Gardner, A., Gilbert, L., Gourmelen, N., Groh, A., Gunter, B., Hanna, E., Harig, C., Helm, V., Horvath, A., Horwath, M., Khan, S., Kjeldsen, K. K., Konrad, H., Langen, P. L., Lecavalier, B., Loomis, B., Luthcke, S., McMillan, M., Melini, D., Mernild, S., Mohajerani, Y., Moore, P.,

https://doi.org/10.5194/egusphere-2024-1597
Preprint. Discussion started: 27 June 2024

Mottram, R., Mouginot, J., Moyano, G., Muir, A., Nagler, T., Nield, G., Nilsson, J., Noël, B., Otosaka, I., Pattle, M. E., Peltier, W. R., Pie, N., Rietbroek, R., Rott, H., Sandberg Sørensen, L., Sasgen, I., Save, H., Scheuchl, B., Schrama, E., Schröder, L., Seo, K.-W., Simonsen, S. B., Slater, T., Spada, G., Sutterley, T., Talpe, M., Tarasov, L., van de Berg, W. J., van der Wal, W., van Wessem, M., Vishwakarma, B. D., Wiese, D., Wilton, D., Wagner, T., Wouters, B., Wuite, J., and The IMBIE Team: Mass balance of the Greenland Ice Sheet from 1992 to 2018, Nature, 579, 233–239, https://doi.org/10.1038/s41586-019-1855-2, publisher: Nature Publishing Group, 2020.

Smith, R. S., Mathiot, P., Siahaan, A., Lee, V., Cornford, S. L., Gregory, J. M., Payne, A. J., Jenkins, A., Holland, P. R., Ridley, J. K., and Jones, C. G.: Coupling the U.K. Earth System Model to Dynamic Models of the Greenland and Antarctic Ice Sheets, Journal of Advances in Modeling Earth Systems, 13, e2021MS002 520, https://doi.org/10.1029/2021MS002520, _eprint: https://onlinelibrary.wiley.com/doi/pdf/10.1029/2021MS002520, 2021.

Straneo, F. and Heimbach, P.: North Atlantic warming and the retreat of Greenland's outlet glaciers, Nature, 504, 36–43, https://doi.org/10.1038/nature12854, publisher: Nature Publishing Group, 2013.

Stuecker, M. F., Bitz, C. M., Armour, K. C., Proistosescu, C., Kang, S. M., Xie, S.-P., Kim, D., McGregor, S., Zhang, W., Zhao, S., Cai, W., Dong, Y., and Jin, F.-F.: Polar amplification dominated by local forcing and feedbacks, Nature Climate Change, 8, 1076–1081, https://doi.org/10.1038/s41558-018-0339-y, publisher: Nature Publishing Group, 2018.

Tebaldi, C., Debeire, K., Eyring, V., Fischer, E., Fyfe, J., Friedlingstein, P., Knutti, R., Lowe, J., O'Neill, B., Sanderson, B., van Vuuren, D., Riahi, K., Meinshausen, M., Nicholls, Z., Tokarska, K. B., Hurtt, G., Kriegler, E., Lamarque, J.-F., Meehl, G., Moss, R., Bauer, S. E., Boucher, O., Brovkin, V., Byun, Y.-H., Dix, M., Gualdi, S., Guo, H., John, J. G., Kharin, S., Kim, Y., Koshiro, T., Ma, L., Olivié, D., Panickal, S., Qiao, F., Rong, X., Rosenbloom, N., Schupfner, M., Séférian, R., Sellar, A., Semmler, T., Shi, X., Song, Z., Steger, C., Stouffer, R., Swart, N., Tachiiri, K., Tang, Q., Tatebe, H., Voldoire, A., Volodin, E., Wyser, K., Xin, X., Yang, S., Yu, Y., and Ziehn, T.: Climate model projections from the Scenario Model Intercomparison Project (ScenarioMIP) of CMIP6, Earth System Dynamics, 12, 253–293, https://doi.org/10.5194/esd-12-253-2021, publisher: Copernicus GmbH, 2021.

Traxl, D., Boers, N., Rheinwalt, A., and Bookhagen, B.: The role of cyclonic activity in tropical temperature-rainfall scaling, Nature Communications, 12, 6732, https://doi.org/10.1038/s41467-021-27111-z, publisher: Nature Publishing Group, 2021.

van den Broeke, M., Bamber, J., Ettema, J., Rignot, E., Schrama, E., van de Berg, W. J., van Meijgaard, E., Velicogna, I., and Wouters, B.: Partitioning Recent Greenland Mass Loss, Science, 326, 984–986, https://doi.org/10.1126/science.1178176, publisher: American Association for the Advancement of Science, 2009.

Winkelmann, R., Martin, M. A., Haseloff, M., Albrecht, T., Bueler, E., Khroulev, C., and Levermann, A.: The Potsdam Parallel Ice Sheet Model (PISM-PIK) – Part 1: Model description, The Cryosphere, 5, 715–726, https://doi.org/10.5194/tc-5-715-2011, publisher: Copernicus GmbH, 2011.

Zeitz, M., Reese, R., Beckmann, J., Krebs-Kanzow, U., and Winkelmann, R.: Impact of the melt–albedo feedback on the future evolution of the Greenland Ice Sheet with PISM-dEBM-simple, The Cryosphere, 15, 5739–5764, https://doi.org/10.5194/tc-15-5739-2021, publisher: Copernicus GmbH, 2021.

Zeitz, M., Haacker, J. M., Donges, J. F., Albrecht, T., and Winkelmann, R.: Dynamic regimes of the Greenland Ice Sheet emerging from interacting melt–elevation and glacial isostatic adjustment feedbacks, Earth System Dynamics, 13, 1077–1096, https://doi.org/10.5194/esd-13-1077-2022, publisher: Copernicus GmbH, 2022.

Zender, C. S.: Analysis of self-describing gridded geoscience data with netCDF Operators (NCO), Environmental Modelling & Software, 23, 1338–1342, https://doi.org/10.1016/j.envsoft.2008.03.004, 2008.

https://doi.org/10.5194/egusphere-2024-1597
Preprint. Discussion started: 27 June 2024

Zhang, Q., Huai, B., Ding, M., Sun, W., Liu, W., Yan, J., Zhao, S., Wang, Y., Wang, Y., Wang, L., Che, J., Dou, J., and Kang, L.: Projections of Greenland climate change from CMIP5 and CMIP6, Global and Planetary Change, 232, 104 340, https://doi.org/10.1016/j.gloplacha.2023.104340, 2024.